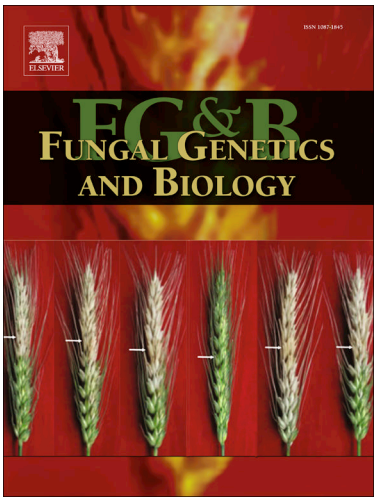

Depletion of the mitotic kinase Cdc5p in *Candida albicans* results in the formation of elongated buds that switch to the hyphal fate over time in a Ume6p and Hgc1p-dependent manner

Amandeep Glory, Chloë Triplet van Oostende, Anja Geitmann, Catherine Bachewich

PII: S1087-1845(17)30130-5
DOI: http://dx.doi.org/10.1016/j.fgb.2017.08.002
Reference: YFGBI 3073

To appear in: *Fungal Genetics and Biology*

Received Date: 18 May 2017
Revised Date: 27 July 2017
Accepted Date: 8 August 2017

Please cite this article as: Glory, A., van Oostende, C.T., Geitmann, A., Bachewich, C., Depletion of the mitotic kinase Cdc5p in *Candida albicans* results in the formation of elongated buds that switch to the hyphal fate over time in a Ume6p and Hgc1p-dependent manner, *Fungal Genetics and Biology* (2017), doi: http://dx.doi.org/10.1016/j.fgb.2017.08.002

Depletion of the mitotic kinase Cdc5p in *Candida albicans* results in the formation of elongated buds that switch to the hyphal fate over time in a Ume6p and Hgc1p-dependent manner.

Amandeep Glory[a], Chloë Triplet van Oostende[b1], Anja Geitmann[b2], and Catherine Bachewich[a*]

[a]Department of Biology, Concordia University, 7141 Sherbrooke St West, Montreal QC, Canada, H4B 1R6

[b]Institut de recherche en biologie végétale, Université de Montréal, 4101 Sherbrooke St E, Montreal, QC, Canada, H1X 2B2

[*]**Corresponding author**: Catherine Bachewich, Department of Biology, Concordia University, catherine.bachewich@concordia.ca

[1]**Present address**: Cell Biology and Image Acquisition Center, Faculty of Medicine, University of Ottawa, 451 Smyth Road, Ottawa, ON, Canada, K1H 8M5, cvanoost@uottawa.ca

[2]**Present address:** Faculty of Agricultural and Environmental Sciences
McGill University, Macdonald Campus, 21111 Lakeshore, Ste-Anne-de-Bellevue
QC, Canada, H9X 3V9, anja.geitmann@mcgill.ca

HIGHLIGHTS

- Hyphal-diagnostic features during a time course of Cdc5p depletion were explored to determine the nature of polarized cells induced by mitotic arrest in *C. albicans*
- Mlc1p and Rga2p showed hyphal patterns but only at later stages of polar growth
- Hyphal-specific gene *UME6* was expressed and impacted late-stage filament morphology

- Polar growth and *UME6* expression in Cdc5p-depleted cells were independent of Hms1p

- Cdc5p depletion thus induces elongated buds that shift to the hyphal fate in a *UME6*-dependent manner

ABSTRACT

The fungal pathogen *Candida albicans* differentiates between yeast, hyphae and pseudohyphae in order to enhance survival in the human host. Environmental cues induce hyphal development and expression of hyphal-specific genes. Filaments also result from yeast cell cycle arrest, but the nature of these cells and their mechanisms of formation are less clear. We previously demonstrated that depletion of the mitotic polo-like kinase Cdc5p resulted in the production of filaments under yeast growth conditions that were distinct from hyphae with respect to several criteria, yet expressed hyphal-specific genes at later stages of development. In order to clarify the identity of these growth forms and their relationship to true hyphae, we conducted time course-based investigations of aspects of the polar growth machinery, which can distinguish cell types. During later stages of Cdc5p depletion, the myosin light chain Mlc1p demonstrated a Spitzenkörper-like localization in the tips of some filaments, and the Cdc42p GAP Rga2p became hyper-phosphorylated, as in true hyphae. Hyphal-specific genes *HWP1*, *UME6* and *HGC1* were strongly expressed at approximately the same time. *HWP1* expression was dependent on Ume6p, and absence of Ume6p or Hgc1p influenced late-stage filament morphology and integrity. Finally, polarized growth and *UME6* expression in Cdc5p-depleted cells were independent of the transcription factor Hms1p. Thus, depleting Cdc5p generates elongated buds that switch to a hyphal fate over time through a mechanism that involves *UME6* and *HGC1* induction, possibly in response to maintenance of polarized growth. The results expand on the multiple strategies with which *C. albicans* can modulate growth mode and expression of virulence determinants.

KEY WORDS: *Candida albicans*, Cdc5p, polo-like kinase, hyphae, mitosis, hyphal-specific genes expression, UME6

1.0 INTRODUCTION

Candida albicans is an important opportunistic fungal pathogen of humans that exists as a commensal in the gastrointestinal or genitourinary tracts, but can cause a range of infections under immune-compromised conditions (Corner and Macgee, 1997). Mortality rates associated with systemic infections can reach as high as 60% (Boonrasiri et al., 2013). One aspect of *C. albicans* biology that is important for virulence is the ability to differentiate into multiple cell types, including yeast, pseudohyphae, and hyphae. Yeast grow via budding that initiates at the G1/S transition of the cell cycle. Initial bud outgrowth is polar, and associated with a high concentration of actin patches, but switches to an isometric mode near mitosis, when the actin patches disperse evenly around the bud (Staebell and Soll, 1985; Hazan et al., 2002). Bud tips contain a polarisome, which regulates actin filament formation at growth sites (Jones et al., 2010). Later in the cell cycle, polarisome components move to the bud neck, where nuclear division and cytokinesis take place (Sudbery et al., 2004). Pseudohyphae are chains of elongated yeast cells with an extended G2 phase, contain constrictions at septation sites, and are similar to yeast with respect to localization of actin patches, the polarisome, and nuclear division across the bud neck (Sudbery et al., 2004; Sudbery, 2011). Hyphae are distinct in that they maintain polarized growth and actin patches at the tip, undergo the first nuclear division within the germ tube, and lack constrictions at septation sites (Sudbery et al., 2004). Hyphal tips contain a polarisome, but also a proposed vesicle supply center (Crampin et al., 2005), similar to the Spitzenkörper found in hyphal tips of filamentous fungi (Virag and Harris, 2006). The Spitzenkörper is seen as a 3D spot in hyphal tips with FM4-64 staining, or localization of the myosin light chain Mlc1p or other proteins (Crampin et al., 2005; Jones and Sudbery, 2010; Bishop et al., 2010). Hyphae also distinctly show hyperphosphorylation of Rga2p, a GTPase activating protein (GAP) for Cdc42p. This results in Rga2p down-regulation, its

exclusion from the tip, and maintainance of Cdc42p activity. In contrast, Rga2p localizes to the tips of small and medium yeast and pseudohyphal buds (Zheng et al., 2007; Court et al., 2007).

The ability to switch between cell types in different environments of the host is crucial for pathogenesis (Lo et al., 1997; Saville et al., 2003). An understanding of the mechansims that underlie cell differentiation may thus reveal new targets for treating infection. The regulation of the yeast-to-hyphal switch has been extensively investigated, and requires elevated tempertaure in combination with other environmental cues that are mediated by a diversity of signaling pathways (reviewed in Sudbery, 2011). An important target of many signaling pathways is the transcription factor Efg1p (Lo et al., 1997; Stoldt et al., 1997). Efg1p regulates filament formation and expression of several hyphal-specific genes (HSG's), including the cell wall protein Hwp1p. *UME6* is another central regulator of hyphal development and a target of Efg1p. Yeast cells lacking *UME6* initiate but do not maintain hyhal growth, and *UME6* ovexpression drives hyphal formation under yeast growth conditions (Banerjee et al., 2008; Zeidler et al., 2009). Ume6p in turn maintains expression of *HGC1* (Carlisle and Kadosh, 2010), a cyclin-related factor that is specifically expressed in hyphal cells and required for maintaining hyphal growth (Zheng et al., 2004), in part through regulating Ume6p in a post-transcriptional manner (Mendelsohn et al., 2017).

C. albicans yeast cells can also form filaments in the absence of hyphal-inducing environmental cues. True hyphae can form under yeast growth conditions upon aresting cells in G1 phase through depletion of the G1 cyclin Cln3p (Bachewich and Whiteway, 2005a; Chapa y Lazo et al., 2005; Woolford et al., 2016). This may be mediated by Cln3p suppression of hyphal morphogenesis via post-transcriptional inhibition of Ume6p (Mendelsohn et al., 2017). Hyphae also form in the absence of the ubiquitin ligase complex factor Cdc4 (Atir-Lande et al., 2009), also due to post-transcriptional regulation of Ume6p by Cln3p and Hgc1p (Mendelsohn et al., 2017).

Filaments can also form through blocking yeast cells in S, G2 or M phase (Bai et al., 2002; Bachewich et al., 2003, 2005b; Bensen et al., 2005; Andaluz et al., 2006; Shi et al., 2007; Shapiro et al., 2009; Trunk et al., 2009; Chou et al., 2011; Senn et al., 2012; Milne et al., 2014) or by reducing expression of various kinases associated with other essential cell cycle or cell growth functions in *C. albicans*. The latter have been referred to as "Essential Process Impairment" (EPI) filaments (Woodford et al., 2016, 2017). Many of these cells also express HSG's. However, the identity of these filaments and the mechanisms underlying their formation largely remain elusive due to lack of comprehensive characterization and complexity in features. For example, cells arrested in mitosis through depletion of the polo-like kinase Cdc5p resemble hyphae in that they maintain polarized growth, lack contrictions along their lengths, move the nucleus from the mother yeast cell into the tube, and express HSG's, including *UME6* (Bachewich et al., 2003, 2005b). They contain a constriction at the bud neck due to polar growth originating from the yeast bud that emerges prior to the cell cycle block. However, the filaments are also distinct from hyphae in forming independent of Efg1p, and requiring the spindle checkpoint factor Bub2p for maintenance of polar growth (Bachewich et al., 2003; 2005b). Bub2p and the spindle checkpoint factor Mad2p are also required for polar growth under other conditions that arrest mitosis, including depletion of the heat shock factor Hsp90p (Shapiro et al., 2009) or exposure to nocodazole (Bai et al., 2002), respectively, but Bub2p is not required for S phase-arrested filaments (Bachewich et al., 2005b). Further, unlike wild-type hyphae, Cdc5p-depleted cells express HSG's only during later stages of elongation (Bachewich et al., 2003, 2005b). A novel regulatory pathway involving the transcription factor Hms1p mediates Hsp90p-depleted filament formation and *UME6* expression (Shapiro et al., 2012a). In addition, some EPI filaments were only partially dependent on core hyphal regulators, suggesting additional and distinct control of filamentation and HSG expression compared to wild-type filaments (Woodford, 2016, 2017). Collectively, this suggets that filaments that form independent

of environmental cues in *C. albicans* may not be created in a similar manner. Further, their identity and connection with true hyphae remain unknown (Sudbery, 2011).

Here, we further characterize filaments that form in response to a mitotic block induced by Cdc5p depletion in order to clarify their identity and mechanisms of formation. Through conducting the first time-course based investigations of aspects of the polar growth machinery and other hyphal-diagnostic features, we provide evidence that Cdc5p-depleted cells initially represent elongated buds, but switch to the hyphal fate over time in a manner that involves Ume6p and Hgc1p, but is independent of Hms1p. Our results extend the array of mechanisms that *C. albicans* utilizes for modulating growth form and HSG gene expression, which are important for virulence.

2.0 MATERIALS AND METHODS

2.1 *Strains, oligonucleotides, plasmids and culture conditions*

Strains, oligonucleotides and plasmids used in this study are listed in Tables 1-3, respectively. Strains were incubated in synthetic medium (0.67% yeast nitrogen base, 2.0 g adenine, 2.5 g uridine, 2.0 g tryptophan, 1.0 g histidine, 1.0 g arginine, 1.0 g methionine, 1.5 g tyrosine, 1.5 g isoleucine, 7.45 g valine, 1.5 g lysine, 2.5 g phenylalanine, 5.0 g glutamic acid, 10.0 g threonine and 3.0 g leucine per 50 L) containing either 2.0% glucose (SD) or 2.0% sodium succinate (SS) to repress or induce expression from the *PCK1* promoter, respectively (Leuker et al., 1997). Alternatively, SD medium lacking (-MC) or containing (+MC) 2.5 mM methionine and 0.5 mM cysteine was utilized to induce or repress expression from the *MET3* promoter, respectively (Care et al,. 1999). Other strains were grown in rich medium (YPD) containing 1.0% yeast extract, 2.0% peptone and 2.0% dextrose. Media was supplemented with 50 μg/ml of uridine, except when *URA3* prototrophs were selected (Bensen et al., 2002). For hyphal induction, medium was supplemented with 10% fetal bovine serum (Wisent Inc,) and cells were incubated at 37ºC. Pseudohyphae were

induced by incubating cells in YPD or SS medium at 36ºC. For most conditions, strains were grown overnight, diluted into fresh medium to an $O.D._{600nm}$ of 0.1 to 0.2, and collected after indicated times. For growth assays, the $O.D._{600nm}$ was recorded at the indicated time intervals. Samples for RNA or protein analysis were collected at the indicated time points and stored at -80°C until extraction.

2.2 *Strain Construction*

In order to tag the C-terminus of *RGA2* with three copies of the hemagglutinin epitope (HA), an *HA-URA3* casette from plasmid pFA-HA-URA3 (Lavoie et al., 2009) was amplified with oligonucleotides AG4F and AG4R. The product was used as a template in a fusion PCR with oligonucleotides AG52F and AG52R, which contained 100 bp homology to regions lying immediatley upstream and downstream from the stop codon of *RGA2*, respectively. The fusion construct was transformed into strains RM1000 and CB105, resulting in strains AG374 and AG379 respectively. In order to tag the C-terminus of *MLC1* with Green Florescent Protein (GFP), the *GFP-URA3* casette from pFA-GFP-URA3 (Gola et al., 2003) was amplified using oligonucletides AG20F and AG20R, which contained 80 bp homology to regions lying upstream and downstream from the stop codon of *MLC1* respectively, and 20 bp homology to regions flanking *GFP-URA3*. The PCR product was transformed into strains RM1000 and CB105, resulting in strains AG332 and AG240, respectively. In order to create a strain containing a single copy of *CDC5* under the control of the *MET3* promoter in the BWP17 background, one copy of *CDC5* was deleted using the *URA3* blaster method (Fonzi et al., 1993;Bachewich et al., 2003), followed by looping out of the *URA3* marker and selection on 5'-fluorootic acid (Sigma-Aldrich), resulting in strain CDC5-25. To place the second copy of *CDC5* under control of the *MET3* promoter, oligonucleotides HCGS13F and HCGS13R were used to amplify a 636 bp fragment lying upstream of the *CDC5* Start codon, while oligonucleotides HCGS15F and HCGS15R amplified a 514 bp fragment immediately downstream

of the Start site. Oligonucleotides HCGS14F and HCGS14R amplified an *ARG4-MET3* fragment from plasmid pFA-ARG4-MET3 (Gola et al., 2003). The three fragments were combined and the fusion product was amplified with oligonucleotides HCGS13F and HCGS15R. The final construct was transformed into strain CDC5-25, resulting in strain AG509. Alternatively, oligonucletides HC10F and HC10R, which contain 80 bp of homologous sequence up and downstream of the START codon of *CDC5*, respectively, were used to amplify an *ARG4-MET3* cassette from pFA-ARG4-MET3. The product was transformed into strain CDC5-25, resulting in strain AG500. In order to delete *UME6*, oligonucleotides AG15F and AG15R were used to amplify a 620 bp fragment lying upstream of the *UME6* Start codon, while oligonucleotides AG17F and AG17R amplified a 490 bp fragment lying downstream of the Stop codon. Oligonucleotides AG16F and AG16R amplified a *URA3* fragment from plasmid pBS-CaURA3 (A.J.P. Brown). The products were combined in a PCR reaction with oligonucleotides AG15F and AG17R, and the final product was transformed into strain AG500, resulting in strain AG518. The second copy of *UME6* was replaced with a *HIS1*-containing fusion product produced in a similar manner with the exception of utilizing pBS-CaHIS1 (C. Bachewich) with oligonucleotides AG16F and AG16R. The resulting strains included AG530 and AG531. In order to delete *HGC1*, oligonucleotides AG75F and AG75R were used to amplify a 580 bp fragment lying upstream of the *HGC1* Start codon, while oligonucleotides AG76F and AG76R amplified a 670 bp fragment lying downstream of the Stop codon. Oligonucleotides AG77F and AG77R amplified a *URA3* fragment from plasmid pBS-CaURA3. The products were combined and the fusion product was produced with oligonucleotides AG75F and AG76R. The final product was transformed into strains AG500 and 509, resulting in strains AG536 and AG540, respectively. The second copy of *HGC1* was replaced with a *HIS1*-containing fusion product produced in a similar manner with the exception of utilizing pBS-CaHIS1 with oligonucleotides AG77F and AG77R. The resulting strains included AG574 and 577. In order

to delete *HMS1,* oligonucleotides AG88F and AG88R amplified a 680 bp fragment lying upstream of the *HMS1* Start codon, oligonucleotides AG89F and AG89R amplified a 490 bp fragment lying downstream of the Stop codon, and AG90F and AG90R amplified a *URA3* fragment from plasmid pBS-CaURA3. The products were combined and the fusion product was produced with oligonucleotides AG88F and AG89R. The final product was transformed into strains AG500 and 509, resulting in strains AG570 and AG572, respectively. The second copy of *HMS1* was replaced with a *HIS1*-containing fusion product produced in a similar manner with the exception of utilizing pBS-CaHIS1 with oligonucleotides AG90F and AG90R. The resulting strains included AG579-AG581 and AG584-AG585, respectively. In order to produce control strains that were isogenic to deletion strains with respect to markers, pRM100 (pUC19 *URA3+,HIS+;* J. Pla) was transformed into strains AG500 and AG509, resulting in strains AG553 and AG547, respectively. Strains were confirmed for correct integration using PCR with oligonucleotide pairs AG21F and AG21R, (*RGA2*), CaURA3F and AG53R (*MLC1*), CaARG4F and AG2R, HC11F and CaMET3R (*CDC5*), AG19F and AG19R, AG19F and CaHIS1R, HH43F and AG66R (*UME6*), CaURA3F and AG78R, AG78F and CaHIS1R, HH08F and HH08R (*HGC1*), or CaURA3F and AG91R, AG91F and CaHIS1R , AG92F and AG92R (*HMS1*). Deletion strains were also confirmed with Southern blotting, utilizing the DIG Hybridization System (Roche Diagnostics, Mannheim, Germany). gDNA was extracted according to Rose *et al*., 1990. DIG-labeled probes were prepared using oligonucleotides AG93F and AG93R, AG99F and AG99R, AG115F and AG115R to confirm *hms1Δ/Δ, hgc1 Δ/Δ* and *ume6 Δ/Δ* strains respectively.

2.3 *Northern blotting*

Briefly, pellets of cultures were lyophilized (Liu et al., 2010) in a freeze drier (ThermoSavant, ModulyoD) at -50^{o}C. The dried material was ground using a mortar and pestle (Liu et al., 2010).

Powder was transferred to occupy approximately 70-80 µl in an Eppendorf tube, and combined with 1.0 ml of TRI-Reagent. RNA was subsequently extracted as previously described (Mogilevsky et al. 2012). The final RNA pellet was re-precipitated with one tenth the volume of 3M sodium acetate pH 5.3 and three times the volume of 95% ethanol. A total of 20 µg RNA was run on a 1.0 % gel, transferred to Zetaprobe membrane (BioRad), and incubated with ^{32}P-labeled probes (T7 Quick Prime Kit, Amersham Pharmacia Biotech), as previously described (Bachewich et al., 2003; Mogilevsky et al., 2012). Probes consisted of approximately 700-800 bp fragments homologous to the open readings frames of *HMS1*, *UME6*, *HWP1*, *HGC1* and *ACT1*, and were amplified with oligonucleotides AG92F and AG92R, AG101F and AG101R, HHHWP1F and HHHWP1R, HH08F and HH08R, or ACT1-129F and ACT1-104R, respectively. Northern blots were visualized with a phosphoimager (Typhoon Variable Mode Imager, GE Healthcare). Blots were quantified as described previously (Chou et al., 2011).

2.4 *Protein extraction and Western blotting*

Protein extracts were prepared according to Liu *et al*., 2010. Extracted protein was quantified using the Bradford assay (Bio-Rad, Mississauga). For protein samples treated with calf intestinal alkaline phosphatase (CIP) (New England Biolabs), EDTA and sodium vanadate were excluded from the HK extraction buffer. Dephosphorylation of proteins was done using 10U of CIP per 10 ug of protein at 37°C for 90 min. Western blotting was performed as described previously (Chou et al., 2011). Briefly, 20 µg of protein was loaded onto SDS-PAGE gels and proteins were transferred to a polyvinylidene difluoride (PVDF) membrane (BioRad). Membranes were blocked with Tris-buffered saline–Tween (TBST; Tris [pH 7.5], 137 mM NaCl, 0.1% Tween 20) containing 5% skim milk for 1 h. Blots were washed three times for 15 min in TBST and incubated for 1.5 h in 0.4 µg/ml anti-HA antibody (12CA5; Roche) diluted in TBST. Blots were rinsed three times for 15

min in TBST and incubated for 1 h in a 1:10,000 dilution of horseradish peroxidase-conjugated anti-mouse secondary antibody (KPL). After washing, blots were developed using Amersham ECL Western blotting analysis system (GE Healthcare). Blots were stripped and incubated with 0.2 μg/ml of anti-PSTAIRE (Santa Cruz Biotechnology) as a loading control. Western blots were quantified using ImageJ as described previously (Chou et al., 2011).

2.5 *Cell staining and imaging*

Cells were stained with filipin (F9765, Sigma) according to Martin and Konopka, 2004. Briefly, freshly-dissolved filipin was added to 1.0 ml of cell culture to a final concentration of 0.01mg/ml. Cultures were incubated for a further 10 min at room temperature in the dark, centrifuged for 1.0 min at 10,000 rpm, and washed with sterile water. Cells were then mounted on slides and immediately examined on a Leica DM6000B microscope (Leica Microsystems Canada Inc., Richmond Hill, ON, Canada) equipped with a Hamamatsu-ORCA ER camera (Hamamatsu Photonics, Hamamatsu City, Japan) using either HCX PL APO 63x NA 1.40-0 oil or HCX PLFLUO TAR 100x NA 1.30-0.6 oil objectives and the DAPI (460-nm) filter. Images were captured with either Openlab software (Improvision Inc., Perkin-Elmer, Waltham, MA) or Volocity (Improvision Inc., Perkin-Elmer, Waltham, MA). Propiodium iodide staining was carried out as previously described (Bachewich et al., 2005b). In order to visualize Mlc1p-GFP, liquid cultures of strain AG240 were first incubated in SS medium at 30°C overnight, washed with sterile water, diluted to a final $O.D._{600nm}$ of 0.2 in fresh SS medium and incubated for 6 h at 30°C to produce yeast cells, 6 h at 36°C to form pseudohyphae, or 2 h at 37°C with the inclusion of 10% calf serum to induce hyphae. In order to repress *CDC5*, overnight cultures were diluted into SD medium to a final $O.D._{600nm}$ of 0.2 and incubated at 30°C for various times. Cultures were centrifuged at 3000 rpm for 1 min and media was removed until approximately 100 μl remained. Cells were

resuspended, mounted on microscope slides and immediately visualized on the Leica DM6000B microscope, utilizing a GFP filter (chroma HQ41020 Narrow-band EGFP) and HCX PL APO 63x NA 1.40-0 oil or HCX PLFLUO TAR 100x NA 1.30-0.6 oil objectives. Alternatively, resuspened cells were mounted on a premade 2% ultrapure low melting point agarose (Invitrogen) pad on a microscope slide, onto which a coverslip was applied and sealed with VALAP (1:1:1 Vaseline: Laonolin: Paraffin). Slides were immediately visualized with a Zeiss Confocal LSM 510 META/LSM 5 LIVE microscope, fitted with a Plan Apochromat 63/1.4 oil DIC objective (pixel size of 0.109 μm). Mlc1p-GFP was observed using the 488nm diode laser and a LP505 emission filter. Mlc1p-GFP localization was similarly observed when overnight cultures of cells were alternatively washed, diluted to a final O.D. of 0.1 in selected media, applied to a premade agar pad on a microscope slide, which was then placed in moist chambers in incubators at the required temperatures. At set times, a slide was removed, fitted with a cover slip as described, and immediately observed on the Zeiss Confocal microscope. For time-lapse imaging of Mlc1p-GFP, ovrenight cultures of cells were diluted into SD medium, applied to the agar pad and sealed as described, then mounted on the Zeiss Confocal microscope. Images were recorded every 30 min, and Z-stacks with a 0.1 μm step were acquired. In order to localize Mlc1p-GFP and FM4-64 (Invitrogen) simultaneously, the dye was added to culture to a final concentration of 40 μM (Crampin et al., 2010) and cells were immediately mounted on microscope slides containing agar pads. Mlc1p-GFP and FM4-64 labelling were visualized on the Zeiss Confocal LSM 510 microscope using the 488nm diode laser (100 mW) with a BP 500-525 emission filter and the 532nm diode laser with a LP 650 emission filter. In order to obtain 3D images and carry out surface rendering of Mlc1p organization in the tips of cells, Z-stacks with a 0.1 μm step acquired with the Zeiss Confocal LSM 510 META/LSM 5 LIVE microscope and the surface rendering module of IMARIS 7.3 software (Bitplane, Switzerland, www.bitplane.com) were utilized. The 3D

volume rendering was applied equally for all pictures. .The thresholding was based on local contrast; for the Spitzenkörper, a diameter of the largest sphere was equivalent to 0.9 μm without smoothing (surface grain of 0.217μm), whereas for the filament tube, a smoothing was applied (surface area detail level of 0.5 μm).

3.0 RESULTS

3.1 Enriched filipin staining is present in tips of Cdc5p-depleted filaments but also in incipient buds of yeast and pseudohyphae

The identity of highly elongated filaments that form independent of environmental cues in *C. albicans*, including Cdc5p-depleted filaments, is unclear due to complexity in features (Bachewich et al., 2003; 2005b). Since Cdc5p-depleted filaments showed expression of HSG's but only later in development, we hypothesized that they may initially be elongated buds that switch to the hyphal fate over time. In order to test this hypothesis, we characterized aspects of the associated polar growth machinery. Previous work demonstrated that tips of hyphae, but not yeast or pseudohyphae, contain enriched lipid rafts visualized with filipin stain (Martin and Konopka, 2004). If filaments produced through Cdc5p depletion were originally elongated yeast buds that switched to a hyphal fate over time, filipin was predicted to be present at the tips but only at a later time point. To test this, overnight cultures of *CDC5* conditional (*cdc5::hisG/cdc5::HIS1 PCK1::CDC5-hisG*) and control (*CDC5/CDC5*) strains were diluted into repressing medium (SD) and incubated at 30°C for 0, 2, 4 or 6 h. The control strain was also incubated in SD medium containing 10% serum at 37°C to induce hyphae, or in SD medium at 36°C to trigger formation of pseudohyphae. Cells were then stained with filipin and visualized. In serum-induced cells, filipin was observed as an enriched signal in the tips of the majority of hyphae (Table 4, Fig.1), as previously reported (Martin and Konopka, 2004). In comparison, cells depleted of Cdc5p for 2 h showed homogeneous staining

on the cell periphery but enriched signal at tips of yeast buds (Fig. 1). By 4-6 h of Cdc5p depletion, when the majority of cells were elongated, an enriched filipin signal was observed at the tips (Table 4). At similar time points, 100% of control cells were in the yeast form at various stages of budding. However, the majority of small to medium-sized yeast buds at later time points also showed enriched filipin signal. A localized spot of the filipin signal was observed in some yeast cells lacking buds, possibly corresponding to the incipient bud site, and control cells grown under pseudohyphal conditions also showed enriched filipin signal at the tips of small and medium-sized buds (Fig. 1). These findings differ from that previously reported for yeast cells of *C. albicans* (Martin and Konopka, 2004). This may be due to the fact that filipin is a complex mixture of several compounds, and we used filipin vs filipin III in the previous study. We also noted that enriched signal at growing tips, including those of yeast buds, was observed only when the filipin solution was freshly prepared from powder. If thawed from a dissolved master stock, only the cell periphery would stain in a homogeneous manner. Thus, these results suggest that enriched filipin signal can be found at polar growth sites in diverse cell types of *C. albicans*. Similarly, filipin signal is enriched at yeast bud tips of *Cryptococcus neoformans,* as well as its mating projections (Nichols et al., 2004), and in growing tips of *S. pombe* yeast cells (Wachtler et al., 2003).

3.2 The myosin light chain Mlc1p is localized in a hyphal-specific manner in a proportion of Cdc5p-depleted cells

Previous work demonstrated that tips of *C. albicans* hyphae were distinct from those of yeast or pseudohyphal buds in that they contained a vesicle supply center or Spitzenkörper, similar to that found in tips of hyphae in filamentous fungi (Crampin et al., 2005; Harris, 2009). The Spitzenkörper in *C. albicans* hyphae was visualized as an FM4-64-staining, 3D spot just distal to or at the tip. The myosin light chain Mlc1p, the Rab GTPase Sec4p and its guanine nucleotide

exchange factor, Sec2p, co-localize to this spot and are simultaneously found at subapical sites of septation (Crampin et al., 2005; Jones and Sudbery, 2010). In contrast, these factors initially localize as a crescent at the tips of growing yeast and pseudohyphal buds, then re-localize to the bud neck prior to septation (Jones and Sudbery, 2010). In order to clarify the identity of Cdc5p-depleted cells and elucidate mechanisms associated with their polarized growth, we explored the localization and organization of Mlc1p. *MLC1* was tagged at the C-terminus with GFP in cells containing a single copy of *CDC5* under control of the *PCK1* promoter (*cdc5*Δ*::hisG/PCK1::CDC5::HIS1, MLC1/MLC1-GFP-URA3*) (Fig. S1). We first investigated whether Mlc1p-GFP localized in the predicted manner under hyphal and yeast conditions. Cells were incubated in *CDC5*-inducing medium (SS) overnight, washed and diluted into fresh SS medium containing 10% serum and incubated at 37º C to induce hyphae, or in SS medium without serum at 30°C to produce yeast. Under hyphal-inducing conditions, Mlc1p-GFP localized as a spot in the tips of germ tubes. FM4-64 staining of hyphal tips proved difficult, but in some hyphae a spot at the tip colocalized with that of Mlc1p-GFP (Fig. 2A). In yeast cells, Mlc1p-GFP localized either as a crescent in bud tips, or at the bud neck (Fig. 2A). Thus, Mlc1p-GFP localized in a predictable manner.

We next explored the localization of Mlc1p-GFP in cells depleted of Cdc5p. After incubating the same strain in repressing medium (SD) at 30°C for 4 h, most cells were elongated with a mean length of 16.8 μm ± 0.6 (s.e.m., n=100). However, approximately 30% of cells contained a spot-like pattern of Mlc1p-GFP at the tips (Fig. 2A, Table 5). Most of these cells demonstrated simultaneous Mlc1p-GFP localization in subapical regions, either at the bud neck or along the long axis of the filament, the latter of which could indicate deregulated attempts at septation (Fig. 2A). The remaining cells showed Mlc1p-GFP at the tip in the form of a crescent and/or at the bud neck, or did not contain a signal (Table 5). In order to determine whether the frequency of cells containing spots of Mlc1p-GFP in the tip increased over time, we next analyzed Mlc1p-GFP in cells

depleted of Cdc5p for 12 h. The total number of cells showing signal was reduced, but approximately 20% contained a spot pattern of Mlc1p-GFP at the tips (Table 5). The spot was dynamic and would rapidly disappear with longer exposure time, comparable to that reported for Mlc1p-YFP in hyphal cells (Crampin et al., 2005, Jones and Sudbery, 2010). Co-localization of Mlc1p-GFP with FM4-64 was not frequent, but observed in some tips (Fig. 2B). In order to confirm that the tip-localized spot of Mlc1p-GFP was in a 3D organization, a 3D surface rendering of confocal image stacks was utilized. The results demonstrate that the spots were present in all focal planes and corresponded to a 3D structure at the tip, similar to that found in serum-induced hyphae (Fig. 2C) (Crampin et al., 2005). The mean volume of Mlc1p-GFP spots in Cdc5p-depleted cell tips was also similar to that in hyphae (Fig. 2C). 3D rendering confirmed the crescent organization of Mlc1p-GFP in other tips of Cdc5p-depleted cells (Fig. 2C). Thus, a proportion of Cdc5p-depleted cells show hyphal-specificity in Mlc1p-GFP localization. In order to obtain more refined information on the temporal dynamics of localization, Mlc1p-GFP was visualized in live cells over a time course of *CDC5* repression. By 2 h, when cells were still in the yeast form and contained buds, Mlc1p-GFP was only detected at some bud necks (Fig. 2Da). At 3 h, some cells were polarized and displayed Mlc1p-GFP signal at the tips that was maintained for the duration of the time course (Fig. 2Dc-j). Z-stack analysis of the tips at higher magnification at each time point confirmed that Mlc1p-GFP was in the form of a spot in some filaments. In some cells, Mlc1p-GFP simultaneously appeared in subapical regions as short bands parallel to the long axis of the Cdc5p-depleted filaments (Fig. 2De). The bands of Mlc1p-GFP would then localize perpendicular to the filament axis, resembling that of an unconstricted septum (Fig. 2Dg-i). In other tips, Mlc1p-GFP was observed in a crescent organization (Fig. 2Dj, l) or no signal was present. Collectively, these results demonstrate that at least a sub-population of Cdc5p-depleted cells show hyphal-specificity in Mlc1p-GFP organization. This feature does not appear to be associated with initial stages of

polarized growth, supporting the hypothesis that the cells may be elongated buds that can change to the hyphal fate over time.

3.3 The Cdc42p GAP Rga2p shows an increase in phosphorylation and decrease in abundance during later stages of Cdc5p depletion

Previous work demonstrated that Cdc28p/Hgc1p-dependent phosphorylation and down-regulation of the Cdc42p GAP, Rga2p, were required for hyphal growth (Zheng et al., 2007; Court and Sudbery, 2007). This phosphorylation correlates with exclusion of Rga2p-GFP from the tips. In contrast, Rga2p-GFP is present in the tips of yeast and pseudohyphal buds. An increase in Rga2p phosphorylation occurs during initial yeast bud outgrowth, but this is transient and independent of Hgc1p (Zheng et al., 2007). In order to further address the identity of Cdc5p-depleted cells, we tagged *RGA2* at the C-terminus with three copies of hemmagglutinin (HA), resulting in strains *RGA2/RGA2-HA-URA3* and *cdc5::hisG/cdc5::HIS1 PCK1::CDC5-hisG, RGA2/RGA2-HA-URA3* (Fig. S2). Overnight cultures of cells grown in SS inducing medium were diluted into fresh SS or SD repressing medium and incubated for various time periods at 30°C. In SD medium, Rga2p-HA demonstrated a shift to a higher molecular weight by 6-7.5 h of Cdc5p depletion (Fig. 3A). In contrast, Rga2p-HA in control cells was not modified (Fig. 3A). In order to determine whether the band shift was due to an increase in phosphorylation, the experiment was repeated in the presence or absence of calf intestinal phosphatase (CIP). When cells were incubated in repressing medium for 9 h, the Rga2p-HA band shift in Cdc5p-depleted cells was suppressed in the presence of CIP (Fig. 3B). Rga2p-HA in control cells showed some CIP-dependent size reduction, suggesting a basal level of phosphorylation, but this was minor compared to that observed in Cdc5p-depleted cells. Intriguingly, cells lacking Cdc5p also showed a decrease in the abundance of Rga2p-HA over time. In order to distiguish whether this was due to a decrease in

protein expression/stability vs. differences in gel loading, samples were run on a high concentration gel that allowed for detection of the lower molecular weight loading control protein Cdc28p. In repressing medium, a decrease in Rga2p-HA intensity was observed at later time points, in contrast to that observed in control cells. The Cdc28p signal did not decrease over time, indicating that the difference in Rga2p-HA signal was not due to issues in loading (Fig. S3). Moreover, the Rga2p-HA signal did not decrease over time when cells were incubated in *CDC5*-inducing medium (Fig. S3), indicating that the effect was specific to depletion of Cdc5p. Thus, in the absence of Cdc5p, Rga2p is modified at the level of phosphorylation but also stability and/or expression. The net effect-downregulation of activity-is similar to that observed in true hyphae, where Rga2p is only hyperphosphorylated. However, this occurs during later stages of *CDC5* repression, consistent with the hypothesis that the filaments may be elongated buds that switch to a hyphal fate over time.

3.4 A core regulator of hyphal growth, *UME6,* and other HSG's including *HGC1* and *HWP1,* are induced in Cdc5p-depleted cells at or near hyphal-specific levels

Ume6p is a core regulator of hyphal growth, as it controls many hyphal-specific genes, and high levels of expression are sufficient to drive hyphal growth from yeast cells (Zeidler et al., 2007; Banergee et al., 2008). Our previous work involving time course-based transcription profiles of Cdc5p-depleted cells demonstrated that *UME6* and other HSGs such as *HGC1* and *HWP1* were induced but only at later stages (Bachewich et al., 2005b). However, HSG's can also be expressed in pseudohyphae, albeit at levels lower than those in hyphae (Berman, 2006, Banergee et al., 2008; Carlise and Kadosh, 2013). In order to clarify whether expression levels of *UME6*, *HWP1* and *HGC1* in Cdc5p-depleted cells were similar to those in hyphae, Northern blots were utilized to quantify expression during a time course of *CDC5* repression. Overnight cultures of *CDC5*-conditional and control strains were diluted into SD repressing medium and incubated at 30°C for

various time periods. For comparison, wild-type cells were incubated in SD medium at 30°C or 37°C with the addition of 10% serum to obtain yeast and hyphal samples, respectively, or 36°C to induce pseudohyphal growth. In Cdc5p-depleted cells, expression was detectable by 7 h, where levels of *UME6* were higher than those of *HGC1* or *HWP1* (Fig. 4). Expression levels of all three genes continued to increase such that by 9-11 h of *CDC5* repression, they were at or near those in established hyphae incubated in serum for 2 h (Fig. 4), and significantly higher than in pseudohyphae (Fig. S4). Intriguingly, the period of HSG induction in Cdc5p-depleted cells correlated with that of Rga2p modifications, suggesting that major changes took place in the cells at this time, and that these are consistent with features of true hyphae.

3.5 Ume6p influences expression of *HWP1* as well as morphology and integrity of Cdc5p-depleted filaments at later stages of growth

If Cdc5p-depleted cells were elongated buds that adapted a hyphal fate over time, we predict that a regulator(s) of hyphal development should influence late stage Cdc5p-depleted growth and HSG expression. Since Cdc5p-depleted filaments do not require the hyphal signaling pathway component Efg1p (Bachewich et al., 2003), but strongly induce *UME6,* we asked if this expression was required for hyphal-specific features observed in the cells. In order to address this question, both copies of *UME6* were deleted from a *CDC5*-conditional strain (*cdc5::hisG/MET3::CDC5-ARG4, ume6::URA3/ume6::HIS1)* (Fig. S5). Overnight cultures of this and a control strain (*cdc5::hisG/MET3::CDC5-ARG4, UME6/UME6, URA3+ HIS1+)* were diluted into +MC repressing medium and incubated for various periods for morphology determination and RNA extraction. In the absence of *UME6*, depleting Cdc5p resulted in polarized cells (Fig. 5). However, morphology was affected in that filament diameters, measured 40 μm from the tip, were wider. This, as well as other features including more branching and vacuolation, became more pronounced with longer periods of

Cdc5p depletion (Table 6, Figs 5, S7). When incubated on solid repressing medium for 30 h, filaments lacking *UME6* also appeared shorter than those of the control strain (Fig. S9). Since more cells lacking *UME6* stained with propidium iodide over time, compraed to control cells, loss of *UME6* also affects cell integrity (Table 7, Fig. S7). We next asked if Ume6p was required for expression of *HWP1* in Cdc5p-depleted cells. Northen blots of RNA obtained from strains incubated in repressing medium for 11 h demonstrated that *HWP1* expression was severly reduced in the absence of *UME6* (Fig. 6). *HGC1* expression was also reduced, but to a lesser extent (Fig. 6). Thus, Ume6p can influence the morphology of Cdc5p-depleted cells, but predominantly during later stages of growth. Ume6p is also important for expression of *HWP1* and, to a lesser extent, *HGC1*, in these cells.

Since *HGC1* was also induced in Cdc5p-depleted cells, we asked if it influenced the Cdc5p-depleted cell phenotype. Both copies of *HGC1* were deleted from a *CDC5* conditional strain, resulting in strain *cdc5::hisG/MET3::CDC5-ARG4, hgc1::URA3/hgc1::HIS1* (Fig S6). In the absence of *HGC1*, Cdc5p-depleted cells could polarize and morphology was similar to control cells at early stages of growth (Fig. 5). However, cells were shorter, wider, more vacuolated, and stained more readily with propidium iodide with longer periods of Cdc5p depletion (Figs. 5, S7, S9) (Tables 6,7), although not as greatly as with absence of *UME6*. Absence of *HGC1* did not affect *HWP1* or *UME6* expression (Fig. 6), similar to that reported in true hyphae (Zheng et al., 2004).

Thus, Ume6p and Hgc1p are important for morphology and integrity of later-stage Cdc5p-depleted filaments. Ume6p is also required for expression of *HWP1* and, in part, *HGC1*. Since true hyphae show similar features, the results support the model that Cdc5p-depleted cells may switch to the hyphal fate over time in a manner dependent in part on the hyphal regulators Ume6p and Hgc1p.

3.6 Cdc5p-depleted cells do not require Hms1p for polarized growth or expression of *UME6* and *HWP1*

The regulation of *UME6* is complex and not fully understood (Carlisle et al., 2009). Under hyphal-inducing conditions, its expression is controlled by transcription factors, such as Efg1p, that are under control of various environmental signaling pathways (Biswas et al., 2007; Sudbery, 2011). Since Cdc5p-depleted cells adapt a hyphal fate at later stages of growth in the absence of hyphal-inducing environmental cues, the mechanisms underlying *UME6* induction in these cells remain unclear. One possibility is a signaling pathway involving the transcription factor Hms1p, which was shown to link the heat shock protein Hsp90p to filamentous growth and expression of HSG's (Shapiro et al., 2012a). Hms1p binds promoters of five HSG's, including *UME6*, and its absence prevents polarized growth and strongly reduces *HWP1* and *UME6* expression in Hsp90p-compromsed cells (Shapiro et al., 2012a). In order to determine whether the Cdc5p-depleted cell phenotype also requires Hms1p, both copies of *HMS1* were deleted from a *CDC5* conditional strain, resulting in strain *cdc5::hisG/MET3::CDC5-ARG4, hms1::URA3/hms1::HIS1* (Fig. S8). In the absence of *HMS1*, Cdc5p-depleted cells were able to grow in a polar manner. Filament morphology and diameter were similar to those of control cells, even at later time points, although some blunt tips were noted (Fig. 7A, Table 6). Filaments were not as vacuolated compared to those lacking Ume6p or Hgc1p (Figs. 5, 7A; Fig. S7), but a moderately higher proportion of cells lacking *HMS1* stained with propidium iodide compared to control cells (Table 7), suggesting some influence on cell integrity. Further, expression of *UME6* or *HWP1* was not reduced in the absence of *HMS1* (Fig. 7B). Thus, Cdc5p-depleted cells grow in a polarized fashion and induce *UME6* and *HWP1* expression via alternate mechanisms.

4.0 DISCUSSION

Arresting yeast cells of *C. albicans* in mitosis results in the formation of filaments that express HSG's, much like true hyphae. However, the identity of these growth forms and the mechanisms underlying their generation have been elusive. Here, we show that filaments produced through depletion of the mitotic polo-like kinase Cdc5p have characteristics of elongated buds during early stages of elongation, but demonstrate several features diagnostic of true hyphae at later growth stages, including Spitzenkörper-like localization of Mlc1p, phosphorylation of the Cdc42p GAP Rga2p, and strong expression of hyphal-associated genes such as *UME6*, *HGC1*, and *HWP1*. *HWP1* expression was strongly dependent on Ume6p, and absence of Ume6p or Hgc1p influenced the maintenance, but not initiation, of filament morphology and integrity. Finally, polar growth and *UME6* expression in Cdc5p-depleted cells were independent of Hms1p, unlike filaments produced through depletion of Hsp90p (Shapiro et al., 2012a). Thus, Cdc5p-depleted filaments may initially represent elongated buds, but switch to the hyphal fate over time through a mechanism that involves *UME6* and *HGC1* induction, possibly in response to maintenance of polar growth.

4.1 Cdc5p-depleted cells are elongated buds during initial stages of polarized growth

We previously suggested that filaments produced through Cdc5p depletion were not hyphae during early growth stages based on their transcription profiles, a requirement for the spindle checkpoint factor Bub2p, and independence of the hyphal regulator Efg1p (Bachewich et al., 2003, 2005b). Our time course-based investigations of aspects of the polar growth machinery support this notion, and suggest that the cells may initially be elongated buds (Bachewich et al., 2005b). Unlike hyphal germ tubes, Cdc5p-depleted cells during early stages of polarized growth did not demonstrate a 3D spot-like localization of Mlc1p-GFP or show hyperphosphorylation of Rga2p (Crampin et al., 2005; Zheng et al., 2007; Court and Sudbery, 2007). Elongated bud formation may

be due to defects in the bud switching from polar to isometric growth. In *S. cerevisiae*, yeast buds grow in a polar manner from G1/S to late G2 phase of the cell cycle, then switch to isometric growth (Pruyne and Bretscher, 2000). The switch is regulated in part by the CDK Cdc28p falling under control of the B-type cyclin Clb2p, which in turn causes disassembly of the Cdc24p-Bem1p-Cla4p complex, a decrease in Cdc42p-GTP, and depolarization of actin patches (Howell and Lew, 2012). In *C. albicans*, yeast buds show similar growth patterns but the precise timing and mechanisms underlying the depolarizing switch are not yet known (Soll et al., 1985; Hazan et al., 2002; Crampin et al., 2010). Since *C. albicans* Cdc5p is required in early mitosis (Bachewich et al., 2003), its absence may influence the depolarization machinery. Consistently, in *S. cerevisiae*, absence of Cdc5p results in a large-budded cell (Hartwell et al., 1973) but overexpression (Song et al., 2000) or mutations that deregulate septin organization or Swe1p function produce elongated buds (Song and Lee, 2001; Park et al., 2003), albeit not as long as those obseved in *C. albicans*. Further, Cdc5p activates Rho1p at the division site, negatively regulates Cdc42p activity in late mitosis to permit cytokinesis, and physically interacts with the Cdc42p GAP Bem3p, demonstrating links between polo-like kinases and cytoskeletal and polarity-regulating factors (Yoshida et al., 2006; Atkins et al., 2013). The polo kinase Plo1p in *S. pombe* also influences new and stress-induced polarized growth (Peterson and Hagan, 2005; Grallert et al., 2013). Although the functions and targets of Cdc5p in *C. albicans* are not yet known, it is possible that Cdc5p depletion deregulates the bud growth pattern, resulting in elongated buds.

4.2 Cdc5p-depleted cells may switch to the hyphal fate in a manner dependent in part on Ume6p and Hgc1p

Since Cdc5p-depleted cells expressed several HSG's at later stages of growth, we previously proposed that they became hyphal-like (Bachewich et al., 2003, 2005). However, pseudohyphae

also express HSG's, albeit at reduced levels (Berman, 2006; Carlisle et al., 2009; Carlisle and Kadosh, 2013). We now provide data that support the model that Cdc5p-depleted cells may switch to the hyphal fate over time. First, Cdc5p-depleted cells express HSG's at later stages of development, including *HWP1*, *UME6* and *HGC1*, at levels approximating those in serum-induced hyphae. Second, the Cdc42p GAP Rga2p shows enhanced phosphorylation at approximately the same time as *UME6* induction. Rga2p hyperphosphorylation is also observed in serum-induced hyphae, which results in down-regulation and a corresponding maintenance of Cdc42p at the hyphal tip (Zheng etal., 2007; Court and Sudbery, 2007). Although Rga2p is hyperphosphorylated in yeast, this is transient and only observed during initial yeast bud outgrowth (Zheng et al., 2007). Since Rga2p was not detectably phosphorylated during early stages of Cdc5p depletion, when the cells were clearly polarizing, the phosphorylation observed at later time points cannot be due to maintenance of phosphorylation associated with incipient bud growth. Cdc5p-depleted cells also showed reduced levels of Rga2p, unlike the situation in serum-induced hyphae. Although novel, this reinforces the net effect of Rga2p down-regulation. This protein depletion was not a global effect, since Cdc28p did not show detectable decreases in abundance during Cdc5p shut-off. Third, absence of Ume6p and a known downstream target, Hgc1p, influenced the morphology with respect to cell diameter and length, as well as the integrity of Cdc5p-depleted cells at later stages of growth, and *HWP1* expression was dependent in large part on Ume6p. That cells could still polarize and grow to some extent without *UME6* or *HGC1* could be due to elongation of the bud with no switch to the hyphal fate. Consistently, Ume6p and Hgc1p are required for maintenance, but not initiation, of serum-induced hyphal growth (Zheng et al., 2004; Banergee et al., 2008). It is also possible that additional regulators contribute to the response, as suggested for EPI filamants (Woodford et al., 2016, 2017). Finally, a proportion of Cdc5p-depleted cells showed hyphal-specific features in Mlc1p-GFP localization, including a 3D spot organization in the tip that could be maintained over

time, and simultaneous localization at the tip and the bud neck or along the subapical region (Crampin et al., 2005). Other cells contained a crescent organization of Mlc1p-GFP in the tip, like pseudohyphae, and by 12 h of Cdc5p depletion, fewer cells contained any signal. The fact that the majority of cells are viable at later stages of *CDC5* repression, based on PI staining, indicates that lack of staining is not due to cell death. Alternatively, it may be due to the dynamic nature of Mlc1p-GFP signal (Crampin et al., 2010) and technical issues associated with capturing Mlc1p-GFP in living cells, as well as potential differences in growth rate due to handling prior to visualization; longer filaments at 12 h post *CDC5* repression are expected to be more sensitive than shorter filaments at 4 h repression. This could also explain why the Mlc1p-GFP data was more heterogeneous than the Rga2p Western blot data. Further, differences in the timing and extent to which a change in fate takes place may underlie the different patterns of Mlc1p during earlier stages of Cdc5p depletion. Although the simultaneous localization of Mlc1p-GFP at the tip and in subapical regions could simply reflect a block in the cell cycle, the 3D spot organization in the tip and unconstricted nature of some subapical bands lying perpendicular to the filament axis implies that the cells were not all simply pseudohyphae. Collectively, the data suggest that Cdc5p-depleted cells can adapt a hyphal fate, under low temperature and low pH conditions.

The mechanisms underlying the delayed emergence of hyphal-specific features in Cdc5p-depleted cells may involve the gradual induction of *UME6* and *HGC1*. Ume6p can regulate the transition from yeast to pseudohyphae to hyphae in a dose-dependent manner (Carlisle et al., 2009, Carlisle and Kadosh, 2013). Maintenance of hyphal growth, but not initiation, requires induction of *UME6*, which in turn maintains expression of HSG's including *HGC1*. Hgc1p/Cdc28p activity in turn is required for Rga2p phosphorylation in true hyphae (Zheng et al., 2007; Court and Sudbery, 2007), and Hgc1p can influence Ume6p at the post-transcriptional level (Mendelsohn et a., 2017). At later stages of Cdc5p-depletion, *UME6* was expressed while Rga2p was phosphorylated,

required for *HWP1* expression, and influenced filament morphogenesis, supporting the idea that its gradual induction may underlie the cell fate change. In one model, expression of *UME6* may induce HSG's, including Hgc1p, which help drive the switch to a hyphal fate. Although it is not known if phosphorylation of Rga2p in Cdc5p-depleted cells requires Hgc1p, it is noteworthy that the timing of *UME6* and *HGC1* induction correlated with that of Rga2p phosphorylation. Down-regulation of Rga2p is not likely to be the initiating cue, since this by itself does not generate filament formation under yeast growth conditions. Rather, yeast cells lacking Rga2p are only somewhat elongated, resembling a bean shape (Zheng et al., 2007, Court and Sudbery, 2007), underscoring Rga2p's role in controlling bud shape. Although *C. albicans* cells lacking both Rga2p and the Cdc42p GAP, Bem3p, demonstrated hyperpolarized growth and some other hyphal features, this was under pseudohyphal growth conditions (Zheng et al., 2007; Court and Sudbery, 2007). It is also possible that several initiating mechanisms are involved, as *HGC1* expression was only partly dependent on Ume6p, as seen in true hyphae (Sudbery 2011), and filamentation from reduced expression of the kinase Cak1p involves several transcriptional regulators (Woodford et al., 2016).

4.3 Induction of *UME6* in the absence of environmental cues or Hms1p suggests additional modes of regulation

A critical question is how depletion of Cdc5p leads to induction of *UME6* and *HGC1*. *UME6* is known to be induced by several environmental hyphal signaling pathway components, such as Efg1p, Tec1p, Cph1p and Eed1p, for example, and is repressed by Nrg1p and Tup1p (Ziedler et al., 2009, Sudbery, 2011). *UME6* is also induced by the transcription factor Hms1p in response to heat treatment or depletion of Hsp90p (Shapiro et al., 2012a). Further, Ume6p is stabilized under several hyphal-inducing conditions, can influence its own expression in a positive feedback loop (Childers et al., 2014; Lu et al., 2013) and is influenced post-transcriptionally by

Hgc1p and Cln3p, where Cln3p has an anatgonizing effect (Mendelsohn et al., 2017). Since Cdc5p-depleted filaments form in the absence of hyphal-inducing cues and Efg1p (Bachewich et al., 2003), do not require Hms1p for polarized growth or *UME6* expression, and do not repress *CLN3*, but rather show a mild induction (Bachewich et al., 2005b), expression of *UME6* in these cells involves alternative mechanisms. Since Cdc5p does not appear to function as a direct repressor of hyphal growth (Bachewich et al., 2003, 2005b), one model could involve maintenance of polarized growth and corresponding changes in actin that in turn influence hyphal gene expression, including *UME6* and *HGC1* (Bachewich et al., 2003, 2005b). Previous work demonstrated that stablized actin can contribute to upregulation of *HWP1* expression in *C. albicans*, G-actin interacts with Cyr1p of the cAMP pathway, and tip localization of Cdc42p is associated with expression of the hyphal transcription program (Wolyniak and Sundstrom, 2007; Bassilana et al., 2005; Zou et al., 2010; Pulver et al., 2013). Maintaining polarized bud growth could thus modify the actin cytoskeleton and associated regulators at the tip over time to a point where they in turn can influence aspects of the hyphal signaling pathways, resulting in a switch to the hyphal fate (Fig. 8). Thus, in addition to the relationship between G1 phase and hyphal development (Bachewich and Whiteway, 2005, Chapa y Lazo et al., 2005; Hussein et al., 2011; Mendelsohn et al., 2017), *C. albicans* may link mitosis to hyphal growth and expression of important virulence factors, albeit utilizing alternative initiating mechanisms.

Linking filamentous growth and associated gene expression patterns to perturbations in yeast cell cycle progression may be physiologically important for *C. albicans.* In the presence of cell cycle stresses within host environments, the response could provide an escape strategy (Gimeno et al., 1992; Bai et al., 2002; Bachewich et al., 2003, 2005b; Gale et al., 2009; Berman, 2006; Woodford et al., 2016). Importantly, reducing expression of the CDK-activating kinase *CAK1* and the resulting filamentous growth was important for biofilm formation, as genes required for biofilm

substrate attachment were expressed (Woolford et al., 2016). The fact that cell cycle checkpoint factors are important for filamentous growth that occurs in response to cell cycle arrest (Bai et al., 2002; Bachewich et al., 2005b, Berman, 2006; Andaluz et al., 2006; Shi et al., 2007; Shapiro et al., 2009), and virulence is attenuated in *C. albicans* strains lacking checkpoint factors such as Mad2p (Bai et al., 2002) or Swe1p (Gale et al., 2009) further support the physiological relevance for a relationship between cell cycle progression and induction of filamentous growth.

In summary, our results shed light on the identity of mitotic-arrested, Cdc5p-depleted cells, and expand on the multiple strategies with which *C. albicans* can modulate growth mode and expression of developmental factors, including *UME6*, which are important for pathogenesis. Since the full repertoire of growth tactics and regulation that *C. albicans* may utilize *in vivo* are not yet clear, it is important to define its various growth forms and understand their mechanisms of formation. To this end, it will be highly informative to determine the direct function of the many cell cycle-associated and other genes that influence filamentation upon manipulation, characterize the filaments to identify common and unique features, and contribute to the growing framework of morphogenesis regulation.

5.0 ACKNOWLEDGEMENTS

The authors thank M. Whiteway for comments on the manuscript. This work was supported by NSERC Discovery Grant N00944 to C. Bachewich. A. Glory was supported by an NSERC PGSD Graduate Student Scholarship.

6.0 REFERENCES

Andaluz, E., Ciudad, T., Gomez-Raja, J., Calderone R. and Larriba G. 2006. Rad52 depletion in *Candida albicans* triggers both the DNA-damage checkpoint and filamentation accompanied by but independent of expression of hypha-specific genes. Mol Microbiol. **59:**1452-1472.
Atir-Lande, A., Gildor, T., Kornitzer, D. 2005. Role for the SCF*CDC4* ubiquitin ligase in *Candida albicans* morphogenesis. Mol Biol Cell. **16:**2772-2785.
Atkins, B.D., Yoshida, S., Saito, K., Wu, C.F., Lew, D.J., Pellman, D. 2013. Inhibition of Cdc42 during mitotic exit is required for cytokinesis. J Cell Biol. **202:**231-240.
Bachewich, C., Thomas, D.Y., Whiteway, M. 2003. Depletion of a polo-like kinase in *Candida albicans* activates cyclase-dependent hyphal-like growth. Mol Biol Cell. **14:**2163-2180.
Bachewich, C., Nantel, A., Whiteway, M. 2005a. Cell cycle arrest during S or M phase generates polarized growth via distinct signals in *Candida albicans*. Mol Microbiol. **57:**942-959.
Bachewich, C., Whiteway, M. 2005b. Cyclin Cln3p links G1 progression to hyphal and pseudohyphal development in *Candida albicans*. Eukaryot Cell. **4:**95-102.
Bai, C., Ramanan, N., Wang, Y.M., Wang, Y. 2002. Spindle assembly checkpoint component CaMad2p is indispensable for *Candida albicans* survival and virulence in mice. Mol Microbiol. **45:**31-44.
Banerjee, M., Thompson, D.S., Lazzell, A., Carlisle, P.L., Pierce, C., Monteagudo, C., Lopez-Ribot, J.L., Kadosh, D. 2008. *UME6,* a novel filament-specific regulator of *Candida albicans* hyphal extension and virulence. Mol Biology Cell. **19:**1354-1365.
Bassilana, M., Hopkins, J., Arkowitz, R.A. 2005. Regulation of the Cdc42/Cdc24 GTPase module during *Candida albicans* hyphal growth. Eukaryot Cell. **4:**588-603.
Bensen, E.S., Clemente-Blanco, A., Finley, K.R., Correa-Bordes, J., Berman, J. 2005. The mitotic cyclins Clb2p and Clb4p affect morphogenesis in *Candida albicans*. Mol Biol Cell. **16:**3387-3400.
Berman, J. 2006. Morphogenesis and cell cycle progression in *Candida albicans*. Curr Opin Microbiol. **9:**595-601.
Bishop, A., Lane, R., Beniston, R., Chapa-y-Lazo, B., Smythe, C., Sudbery, P. 2010. Hyphal growth in *Candida albicans* requires the phosphorylation of Sec2 by the Cdc28-Ccn1/Hgc1 kinase. EMBO J. **29:**2930-2942.
Biswas, S., Van Dijck, P., Datta, A. 2007. Environmental sensing and signal transduction pathways regulating morphopathogenic determinants of *Candida albicans*. Microbiol Mol Biol Rev. **71:**348-376.
Boonyasiri, A., Jearanaisilavong, J., Assanasen, S. 2013. Candidemia in Siriraj Hospital: epidemiology and factors associated with mortality. J Med Assoc Thail. **96**(Suppl 2)**:**S91-97.
Care, R.S., Trevethick, J., Binley, K.M., Sudbery, P.E. 1999. The *MET3* promoter: a new tool for *Candida albicans* molecular genetics. Mol Microbiol. **34:**792-798.
Carlisle, P.L., Banerjee, M., Lazzell, A., Monteagudo, C., Lopez-Ribot, J.L., Kadosh, D. 2009. Expression levels of a filament-specific transcriptional regulator are sufficient to determine *Candida albicans* morphology and virulence. Proc Natl Acad Sci U S A. **106:**599-604.
Carlisle, P.L., Kadosh, D. 2010. *Candida albicans* Ume6, a filament-specific transcriptional regulator, directs hyphal growth via a pathway involving Hgc1 cyclin-related protein. Eukaryot Cell. **9:**1320-1328.
Carlisle, P.L., Kadosh, D. 2013. A genome-wide transcriptional analysis of morphology determination in *Candida albicans*. Mol Biol Cell. **24:**246-260.
Chapa y Lazo, B., Bates, S., Sudbery, P. 2005. The G1 cyclin Cln3 regulates morphogenesis in *Candida albicans*. Eukaryot Cell. **4:**90-94.

Childers, D.S., Mundodi, V., Banerjee, M., Kadosh, D. 2014. A 5' UTR-mediated translational efficiency mechanism inhibits the *Candida albicans* morphological transition. Mol Microbiol. **92:**570-585.
Chou, H., Glory, A., Bachewich, C. 2011. Orthologues of the anaphase-promoting complex/cyclosome coactivators Cdc20p and Cdh1p are important for mitotic progression and morphogenesis in *Candida albicans*. Eukaryot Cell. **10:**696-709.
Ciudad, T., Andaluz, E., Steinberg-Neifach, O., Lue N.F., Gow, N.A., Calderone, R.A., Larriba, G. 2004. Homologous recombination in *Candida albicans*: role of CaRad52p in DNA repair, integration of linear DNA fragments and telomere length. Mol Microbiol. **53:**1177-1194.
Court, H., Sudbery, P. 2007. Regulation of Cdc42 GTPase activity in the formation of hyphae in *Candida albicans*. Mol Biol Cell. **18:**265-281.
Crampin, H., Finley, K., Gerami-Nejad, M., Court, H., Gale, C., Berman, J., Sudbery, P. 2005. *Candida albicans* hyphae have a Spitzenkörper that is distinct from the polarisome found in yeast and pseudohyphae. J Cell Sci. **118:**2935-2947.
Fonzi, W.A., Irwin, M.Y. 1993. Isogenic strain construction and gene mapping in *Candida albicans*. Genetics. **134:**717-728.
Gale, C.A., Leonard, M.D., Finley, K.R., Christensen, L., McClellan, M., Abbey, D., Kurischko, C., Bensen, E., Tzafrir, I., Kauffman, S., Becker, J., Berman. J. 2009. *SLA2* mutations cause *SWE1*-mediated cell cycle phenotypes in *Candida albicans* and *Saccharomyces cerevisiae*. Microbiology. **155:**3847-3859.
Gimeno, C.J., Ljungdahl, P.O., Styles, C.A., Fink, G.R. 1992. Unipolar cell divisions in the yeast S. cerevisiae lead to filamentous growth: regulation by starvation and RAS. Cell **68**: 1077-90.
Gola, S., Martin, R., Walther, A., Dunkler, A., Wendland, J. 2003. New modules for PCR-based gene targeting in *Candida albicans*: rapid and efficient gene targeting using 100 bp of flanking homology region. Yeast. **20:**1339-1347.
Grallert, A., Patel, A., Tallada, V.A., Chan, K.Y., Bagley, S., Krapp, A., Simanis, V., Hagan, I.M. 2013. Centrosomal MPF triggers the mitotic and morphogenetic switches of fission yeast. Nat Cell Biol. **15:**88-95.
Harris, S.D. 2009. The Spitzenkörper: a signalling hub for the control of fungal development? Mol Microbiol. **73:**733-736.
Hazan, I., Sepulveda-Becerra M., Liu H. 2002. Hyphal elongation is regulated independently of cell cycle in *Candida albicans*. Mol Biol Cell. **13:**134-145.
Howell, A.S., Lew, D.J. 2012. Morphogenesis and the cell cycle. Genetics. **190:**51-77.
Jones, L.A., Sudbery, P.E. 2010. Spitzenkörper, exocyst, and polarisome components in *Candida albicans* hyphae show different patterns of localization and have distinct dynamic properties. Eukaryot Cell. **9:**1455-1465.
Lavoie, H., Sellam, A., Askew, C., Nantel, A., Whiteway, M. 2008. A toolbox for epitope-tagging and genome-wide location analysis in *Candida albicans*. BMC Genomics. **9:**578.
Leuker, C.E., Sonneborn, A., Delbruck, S., Ernst, J.F. 1997. Sequence and promoter regulation of the *PCK1* gene encoding phosphoenolpyruvate carboxykinase of the fungal pathogen *Candida albicans*. Gene. **192:**235-240.
Liu, H.L., Osmani, A.H., Ukil, L., Son, S., Markossian, S., Shen, K.F., Govindaraghavan, M., Varadaraj, A., Hashmi, S.B., De Souza, C.P., Osmani, S.A. 2010. Single-step affinity purification for fungal proteomics. Eukaryot Cell. **9:**831-833.
Lo, H.J., Kohler, J.R., DiDomenico, B., Loebenberg, D., Cacciapuoti, A., Fink, G.R. 1997. Nonfilamentous *C. albicans* mutants are avirulent. Cell. **90:**939-949.

Lu, Y., Su, C., Solis, N.V., Filler, S.G., Liu, H. 2013. Synergistic regulation of hyphal elongation by hypoxia, CO_2, and nutrient conditions controls the virulence of *Candida albicans*. Cell Host Microbe. **14:**499-509.
Martin, S.W., Konopka, J.B. 2004. Lipid raft polarization contributes to hyphal growth in *Candida albicans*. Eukaryot Cell. **3:**675-684.
Mendelsohn, S., Pinsky, M., Weissman, Z. and Konitzer, D. 2017. Regulation of the *Candida albicans* Hypha-Inducing Transcription Factor Ume6 by the CDK1 Cyclins Cln3 and Hgc1. mSphere **2**, 1-13. **Milne, S.W., Chatham, J., Lloyd, D., Shaw, S., Moore, K., Paszkiewicz, K.H., Aves, S.J., Bates S.** 2014. Role of *Candida albicans* Tem1p in mitotic exit and cytokinesis. Fungal Genet. Biol. **69**: 84-95. **Mogilevsky, K., Glory, A., Bachewich, C.** 2012. The Polo-like kinase *PLKA* in *Aspergillus nidulans* is not essential but plays important roles during vegetative growth and development. Eukaryot Cell. **11:**194-205.
Nichols, C.B., Fraser, J.A., Heitman, J. 2004. PAK kinases Ste20 and Pak1 govern cell polarity at different stages of mating in *Cryptococcus neoformans*. Mol Biol Cell. **15:**4476-4489.
Ofir, A., Hofmann, K., Weindling, E., Gildor, T., Barker, K.S., Rogers, P.D., Kornitzer, D. 2012. Role of a *Candida albicans* Nrm1/Whi5 homologue in cell cycle gene expression and DNA replication stress response. Mol Microbiol. **84:**778-794.
Odds, F.C. 1985. Morphogenesis in *Candida albicans*. Crit Rev Microbiol. **12:**45-93.
Park, C.J., Song, S., Lee, P.R., Shou, W., Deshaies, R.J., Lee, K.S. 2003. Loss of *CDC5* function in *Saccharomyces cerevisiae* leads to defects in Swe1p regulation and Bfa1p/Bub2p-independent cytokinesis. Genetics. **163:**21-33.
Petersen, J., Hagan I.M. 2005. Polo kinase links the stress pathway to cell cycle control and tip growth in fission yeast. Nature. **435:**507-512.
Pruyne, D., Bretscher, A. 2000. Polarization of cell growth in yeast. I. Establishment and maintenance of polarity states. J Cell Sci. **113**(Pt 3)**:**365-375.
Pulver, R., Heisel, T., Gonia, S., Robins, R., Norton, J., Haynes, P., Gale, C.A. 2013. Rsr1 focuses Cdc42 activity at hyphal tips and promotes maintenance of hyphal development in *Candida albicans*. Eukaryot Cell. **12:**482-495.
Roemer T., and Krysan D.J. 2014. Antifungal drug development: challenges, unmet clinical needs, and new approaches. Cold Spring Harb. Perspect. Med. **4** (5)
Rose, M.D., Winston, F.M., Hieter, P., Sherman, F.1990. Methods in yeast genetics: a laboratory course manual. Cold Spring Harbor Laboratory Press, Cold Spring Harbor, New York.**Saville, S.P., Lazzell, A.L., Monteagudo, C., Lopez-Ribot, J.L.** 2003. Engineered control of cell morphology *in vivo* reveals distinct roles for yeast and filamentous forms of *Candida albicans* during infection. Eukaryot Cell. **2:**1053-1060.
Senn, H., Shapiro, R.S., Cowen, L.E. 2012. Cdc28 provides a molecular link between Hsp90, morphogenesis, and cell cycle progression in *Candida albicans*. Mol Biol Cell. **23:**268-283.
Shi, Q.M., Wang, Y.M., Zheng, X.D., Lee, R.T., Wang, Y. 2007. Critical role of DNA checkpoints in mediating genotoxic-stress-induced filamentous growth in *Candida albicans*. Mol Biol Cell. **18:**815-826**Shapiro, R.S., Uppuluri, P., Zaas, A.K., Collins, C., Senn, H., Perfect, J.R., Heitman, J., Cowen, L.E.** 2009. Hsp90 orchestrates temperature-dependent *Candida albicans* morphogenesis via Ras1-PKA signaling. Curr Biol. **19:**621-629.
Shapiro, R.S., Sellam, A., Tebbji, F., Whiteway, M., Nantel, A., Cowen, L.E. 2012a. Pho85, Pcl1, and Hms1 signaling governs *Candida albicans* morphogenesis induced by high temperature or Hsp90 compromise. Curr Biol. **22:**461-470.
Shapiro, R.S., Zaas, A.K., Betancourt-Quiroz, M., Perfect, J.R., Cowen, L.E. 2012b. The Hsp90 cochaperone Sgt1 governs *Candida albicans* morphogenesis and drug resistance. PloS One. **7:**e44734.

Soll, D.R., Herman, M.A., Staebell, M.A. 1985. The involvement of cell wall expansion in the two modes of mycelium formation of *Candida albicans*. J Gen Microbiol. **131:**2367-2375.
Song, S., Grenfell, T.Z., Garfield, S., Erikson, R.L., Lee, K.S. 2000. Essential function of the polo box of Cdc5 in subcellular localization and induction of cytokinetic structures. Mol Cell Biol. **20:**286-298.
Song, S., Lee, K.S. 2001. A novel function of *Saccharomyces cerevisiae CDC5* in cytokinesis. J Cell Biol. **152:**451-469.
Staebell, M., Soll, D.R. 1985. Temporal and spatial differences in cell wall expansion during bud and mycelium formation in *Candida albicans*. J Gen Microbiol. **131:**1467-1480.
Stoldt, V.R., Sonneborn, A., Leuker, C.E., Ernst, J.F. 1997. Efg1p, an essential regulator of morphogenesis of the human pathogen *Candida albicans*, is a member of a conserved class of bHLH proteins regulating morphogenetic processes in fungi. EMBO J. **16:**1982-1991.
Sudbery, P., Gow, N., Berman, J. 2004. The distinct morphogenic states of *Candida albicans*. Trends Microbiol. **12:**317-324.
Sudbery, P.E. 2011. Growth of *Candida albicans* hyphae. Nat Rev Microbiol. **9:**737-748.
Trunk, K., Gendron, P., Nantel, A., Lemieux, S. Roemer, T., and Raymond, M. 2009. Depletion of the cullin Cdc53p induces morphogenetic changes in *Candida albicans*. Eukaryot Cell **8,** 756-767.
Virag, A., Harris, S.D. 2006. The Spitzenkörper: a molecular perspective. Mycol Res. **110:**4-13.
Wachtler, V., Rajagopalan, S. and Balasubramanian, M.K. 2003. Sterol rich plasma membrane domains in the fission yeast *Schizosaccahromyces pombe*. J Cell Sci. **116**: 867-874.
Whiteway, M., Bachewich, C. 2007. Morphogenesis in *Candida albicans*. Annu Rev Microbiol. **61:**529-553.
Wolyniak, M.J., Sundstrom, P. 2007. Role of actin cytoskeletal dynamics in activation of the cyclic AMP pathway and *HWP1* gene expression in *Candida albicans*. Eukaryot Cell. **6:**1824-1840.
Woodford, C.A., Lagree, K., Xu, W., Aleynikov, T., Adhikari, H., Sanchez, H., Cullen, P.J., Lanni, F., Andes, D.R., Mitchell, A.P. 2016. Bypass of *Candida albicans* Filamentation/ Biofilm Regulators through Diminished Expression of Protein Kinase Cak1. PLOS Genet **12**(12):e1006487.
Woodford, C.A., Lagree, K., Xu, W., Aleynikov, T., Mitchell, A.P. 2017. Negative control of *Candida albicans* filamentation-associated gene expression by essential protein kinase gene *KIN28*. Curr Genet. May 13 doi: 10.1007/s00294-017-0705-8.
Yoshida, S., Kono, K., Lowery, D.M., Bartolini, S., Yaffe, M.B., Ohya, Y., Pellman, D. 2006. Polo-like kinase Cdc5 controls the local activation of Rho1 to promote cytokinesis. Science. **313:**108-111.
Zeidler, U., Lettner, T., Lassnig, C., Muller, M., Lajko, R., Hintner, H., Breitenbach, M., Bito, A. 2009. *UME6* is a crucial downstream target of other transcriptional regulators of true hyphal development in *Candida albicans*. FEMS Yeast Res. **9:**126-142.
Zheng, X., Wang, Y., Wang, Y. 2004. Hgc1, a novel hypha-specific G1 cyclin-related protein regulates *Candida albicans* hyphal morphogenesis. EMBO J. **23:**1845-1856.
Zheng, X.D., Lee, R.T.H., Wang, Y.M., Lin, Q.S., Wang, Y. 2007. Phosphorylation of Rga2, a Cdc42 GAP, by CDK/Hgc1 is crucial for *Candida albicans* hyphal growth. Embo J. **26:**3760-3769.
Zou, H., Fang, H.M., Zhu, Y., Wang, Y. 2010. *Candida albicans* Cyr1, Cap1 and G-actin form a sensor/effector apparatus for activating cAMP synthesis in hyphal growth. Mol Microbiol. **75:**579-591.

FIGURE LEGENDS

Figure 1: Tips of Cdc5p-depleted cells and young buds of yeast and pseudohyphae show enriched filipin staining, similar to hyphal tips. Overnight cultures of strains AG240 (*cdc5::hisG/cdc5::HIS1 PCK1::CDC5-hisG, MLC1/MLC1-GFP-URA3*) and AG332 (*CDC5/CDC5, MLC1/MLC1-GFP-URA3*) grown at 30°C in inducing medium (SS) were diluted into repressing medium (SD) and incubated at 30°C for the indicated times. Strain AG332 was also incubated in SD medium at 36°C for 6 h to promote pseudohyphal growth or SD medium supplemented with 10% FBS at 37°C for 90 min to induce hyphae. Live cells were stained with filipin for 10 min, washed with sterile water and immediately examined by fluorescence microscopy. Bars:10 μm.

Figure 2: Mlc1p-GFP localization in Cdc5p-depleted cells. (A) Overnight cultures of strain AG240 (*cdc5::hisG/cdc5::HIS1 PCK1::CDC5-hisG, MLC1/MLC1-GFP-URA3*) grown at 30°C in inducing medium (SS) were diluted into fresh SS medium supplemented with 10% FBS at 37°C for 2 h to induce hyphae, SS medium at 30°C for 5 h for yeast growth, or SD repressing medium at 30°C for 4 (third panel) or 6 h (fourth panel) to deplete Cdc5p. Prior to mounting on slides and imaging, FM4-64 was introduced to cell cultures. **(B)** Enhanced magnification of a cell depleted of Cdc5p for 6 h showing co-localization of Mlc1p-GFP and FM4-64 at the tip. Bars:10 μm. **(C)** 3D imaging and volume measurements of Mlc1p-GFP signals in tips of serum-induced hyphae and Cdc5p-depleted cells prepared as described in (A). The surface rendering module of the IMARIS 7.3 software was based on 0.1 μm step Z-stacks. Student T-tests were performed relative to the mean volume of Mlc1p-GFP spots in hyphae. **(D)** Time course of Mlc1p-GFP localization in Cdc5p-depleted cells. Strain AG240 was incubated in SS inducing medium as described in (A), transferred to a pre-made agarose pad consisting of SD repressing medium on a microscope slide,

sealed with VALAP and visualized with LSM 510 confocal microscope fitted with a x 63 objective. Images were recorded every 30 min, and Z stack series consisting of 0.1 μm steps were acquired. The star indicates one tip with a spot of Mlc1p-GFP over time. Tips in (j) designated with an arrow or arrowhead contain a spot or crescent of Mlc1p-GFP, and are shown with higher magnification in (k) and (l), respectively.

Figure 3: Rga2p undergoes a phosphorylation-dependent shift in Cdc5p-depleted cells. **(A)** Western blot of overnight cultures of strains AG374 (*CDC5/CDC5, RGA2/RGA2-HA-URA3*) and AG379 (*cacdc5::hisG/cacdc5::HIS1 PCK1::CaCDC5-hisG, RGA2/RGA2-HA-URA3*) that were grown in SS medium, diluted into SD repressing medium at 30°C and collected at the indicated time points. Strain AG374 was also incubated in SD medium supplemented with 10% Fetal Bovine Serum (FBS) for 2 h at 37°C to induce hyphae. **(B)** Western blot of select protein samples from (A) either in the presence (+) or absence (-) of calf intestinal alkaline phosphatase (CIP).

Figure 4: *UME6, HWP1* and *HGC1* expression is induced at later time points of Cdc5p depletion. Overnight cultures of strains CB400 (*URA3+HIS1+*) and CB104 (*cacdc5Δ::hisG/cacdc5Δ:: HIS1/PCK1::CaCDC5-URA3*) were transferred from SS to SD repressing medium and incubated at 30°C for the indicated time points. Strain SC5314 (+/+) was also grown in either SD medium at 30°C for 8 h to promote yeast growth (Y) or SD medium supplemented with 10% FBS at 37°C for 2 h to induce hyphae (H). *ACT1* was used as loading control, for the two different membranes. Density values represent adjusted relative densities and were calculated using ImageJ as described in Chou *et al.*, 2011.

Figure 5: Absence of *UME6 or HGC1* influences the shape and integrity of Cdc5p-depleted filaments at only later stages of growth. Overnight cultures of strains AG553 (*cdc5Δ::hisG/MET3::CDC5-ARG4, URA3+ HIS1+, UME6/UME6, HGC1/HGC1),* AG530 (*cdc5Δ::hisG/MET3::CDC5-ARG4, ume6Δ::URA3/ume6Δ::HIS1, HGC1/HGC1*) and AG574 (*cdc5Δ::hisG/MET3::CDC5::ARG4, hgc1Δ::URA3/hgc1Δ::HIS, UME6/UME6*) in -MC inducing medium were diluted into +MC repressing medium and incubated at 30°C for 6 or 24 h. Samples at 6 h were fixed in 70% ethanol prior to viewing while 24 h samples were live when mounted on microscope slides. Bars:10 μm.

Figure 6: Expression levels of *HWP1* and *HGC1* are reduced in Cdc5p-depleted cells lacking *UME6*. Overnight cultures of strains AG553, AG547 (*cdc5::hisG/MET3::CDC5-ARG4 URA3+ HIS1+*), AG530, AG531 (*cdc5::hisG/MET3::CDC5-ARG4 ume6::URA3/ume6::HIS1*)and AG574, AG577 (*cdc5::hisG/MET3::CDC5-ARG4 hgc1::URA3/hgc1::HIS1*) were diluted into +MC repressing medium and incubated at 30°C for 11 h. *ACT1* was used as loading control. Density values represent adjusted relative densities and were calculated using ImageJ as described in Chou *et al*., 2011.

Figure 7: Absence of *HMS1* does not prevent polarized growth or expression of *UME6* and *HWP1* in Cdc5p-depleted cells. (A) Overnight cultures of strains AG553 (*cdc5Δ::hisG/MET3::CDC5-ARG4, URA3+ HIS1+, HMS1/HMS1*), and AG580 (*cdc5Δ::hisG/MET3::CDC5-ARG4, hms1Δ::URA3/hms1Δ::HIS1*) were diluted into +MC repressing medium and incubated at 30°C for 6 or 24 h. Samples at 6 h were fixed in 70% ethanol while 24 h samples were observed live under the microscope. Bars:10 μm.

(B) Overnight cultures of strains AG553, AG547 (*cdc5::hisG/MET3::CDC5-ARG, URA3+ HIS1+, HMS1/HMS1)* and AG579, AG580 AG581 (*cdc5::hisG/MET3::CDC5-ARG4 hms1::URA3/hms1::HIS1)* were diluted into +MC repressing medium and incubated at 30°C for 11 h. Strain *SC5314* (+/+) was also grown in +MC medium at either 30°C for 8 h to promote yeast growth (Y) or supplemented with 10% FBS at 37°C for 2 h to induce hyphae (H). *ACT1* was used as loading control. Density values represent adjusted relative densities and were calculated using ImageJ as described in Chou *et al*., 2011.

Figure 8: Model for interplay between Cdc5p depletion and hyphal signaling pathways to generate hyphal filaments from elongated buds. Environmental cues such as heat and serum are mediated by a variety of signaling pathways and transcription factors, including Efg1p, to induce yeast cells to grow into hyphae and express HSG's such as the cell wall protein Hwp1p (black circles on hyphae). Efg1p function is mediated in part through the transcription factor Ume6p and Hgc1p. Ume6p can also induce *HGC1* expression. Ume6p and Hgc1p influence a variety of targets required for hyphal growth and hyphal-specific gene expression. Hgc1p acts with the CDK Cdc28p to phosphorylate Rga2p, which in turn downregulates its activity and contributes to hyphal growth (reviwed in Sudbery, 2011). Depletion of Cdc5p results in a mitotic arrest and elongated bud growth. Continued polarized growth of the bud and changes in actin at the tip feed back on the hyphal signaling program, including *UME6* and *HGC1* expression. Hgc1p may influence Rga2p phosphorylation, and collectively these changes result in a switch to the hyphal fate and HSG expression, including *HWP1*.

Table 1: Strains used in this study

Strain	Genotype	Source
RM1000	*ura3Δ:: imm434/ura3Δ::1 imm434 his1Δ::hisG/his1Δ::hisG*	Negredo *et al*.1997
BWP17	*ura3Δ*::*imm434/ura3Δ*::*imm434 his1Δ*::*hisG/his1Δ*::*hisG arg4Δ*::*hisG/arg4Δ*::*hisG*	Wilson *et al*., 1999
SC5314	*URA3/URA3, HIS1/HIS1*	Fonzi and Irwin, 1993
CB104	*cdc5Δ::hisG/cdc5Δ::HIS1 PCK1::CDC5-URA3*	Bachewich *et al*., 2003
CB105	*cdc5Δ::hisG/cdc5Δ::HIS1 PCK1::CDC5-hisG*	Bachewich *et al*., 2003
CB400	RM1000 (pRM100 *URA3+, HIS1+*)	Bachewich *et al*., 2003
CDC5-25	*CDC5/cdc5Δ::hisG*	This study
AG240	*cdc5Δ::hisG/cdc5Δ::HIS1 PCK1::CDC5-hisG MLC1/MLC1-GFP-URA3*	This study
AG332	*MLC1/MLC1-GFP-URA3*	This study
AG374	*RGA2/RGA2-HA-URA3*	This study
AG379	*cdc5Δ::hisG/cdc5Δ::HIS1 PCK1::CDC5-hisG RGA2/RGA2-HA-URA3*	This study
AG500	*cdc5Δ::hisG/MET3::CDC5-ARG4*	This study
AG509	*cdc5Δ::hisG/MET3::CDC5-ARG4*	This study
AG518	*cdc5Δ::hisG/MET3::CDC5-ARG4, UME6/ume6Δ::URA3*	This study
AG530, 531	*cdc5Δ::hisG/MET3::CDC5-ARG4, ume6Δ::URA3/ume6Δ::HIS1*	This study
AG536, 540	*cdc5Δ::hisG/MET3::CDC5-ARG4, HGC1/hgc1Δ::URA3*	This study
AG547	AG509 pRM100 (*URA3+HIS1+*)	This study
AG553	AG500 pRM100 (*URA3+HIS1+*)	This study
AG574, 577	*cdc5Δ::hisG/MET3::CDC5-ARG4, hgc1Δ::URA3/hgc1Δ::HIS1*	This study
AG570, 572	*cdc5Δ::hisG/MET3::CDC5-ARG4, HMS1/hms1Δ::URA3*	This study
AG579-581	*cdc5Δ::hisG/MET3::CDC5-ARG4, hms1Δ::URA3/hms1Δ::HIS1*	This study

Table 2: Oligonucleotides used in this study

Name	Sequence	Source
AG2R	ATAGTTACGATTAGTGGTGG	This study
AG4F	GGTCGACGGATCCCCGGGTTATACCCATACGATGTTCCTG AC	Lavoie *et al*., 2008
AG4R	TCGATGAATTCGAGCTCGTT	Lavoie *et al*., 2008
AG15F	AGAATTTCCCGGGAGTTGCTTATTATTGAT	This study
AG15R	TGGAAGTAAATTGAGGATATTGATGTTTGG	This study
AG16F	CCAAACATCAATATCCTCAATTTACTTCCATATAGGGCGA ATTGGAGCTC	This study
AG16R	CCGTCAACCGTCAACCTGTTAATTCTTAATGACGGTATCG ATAAGCTTGA	This study
AG17F	ATTAAGAATTAACAGGTTGACGGTTGACGG	This study
AG17R	TAAGGTTTAGACTTTTCCGTATGATGAAAC	This study
AG19F	ATTAGAAACCAACAGAGGAA	This study
AG19R	TTGTCGTAGTTGTTGAACTA	This study
AG20F	ATGAGTTATTAAAAGGGGTCAATGTAACTTCTGATGGAAA TGTGGATTATGTTGAA TTTGTCAAATCAATTTTAGACCAAGGTGCTGGCGCAGGTG CTTC	This study
AG20R	TTGGCATATATTACTCTCCAAAGTAACTTATCAAGTACTA CATAAAACTTCAAATAA ACGGTATCCAATTCGAACAAGACCCGCATAGGCCACTAGT GGA	This study
AG21F	CAAGAAATCATCAACAGACC	This study
AG21R	TCCGTCATCATAATTGGTGC	This study
AG52F	AACTTTAGCGAAGGATGAATCCGGTGTAAAAGAAATGAC CGATATGGGATTTAGAAATGA TACAACAGAGTTACTATTGACAGAATCACATAGAATCTTT GGTCGACGGATCCCCGGGTT	This study
AG52R	TACCCAAAAAACAATTTAATACCATTGAATACTTGATCCG TAATGGACATAGAAAACTAGAA ATGTATCTGAATCCACAACTAAAAGATATTCATTAACATC GATGAATTCGAGCTCGTT	This study
AG53R	CTCTGCCAGGATACTACTTG	This study
AG66R	GTACGTGTGATGATGATGAT	This study
AG75F	AATTCTGTCCTCCTCCCCTCAAAGTTTCTA	This study
AG75R	AAGTGTTGGGTATTGGTTTGATGCTTTGAT	This study
AG76F	GAGAATGGAGAATGGAGAAAGATGTTGTTA	This study
AG76R	GGACGAATAAAGGATACTTTCCAGTAGTGT	This study
AG77F	ATCAAAGCATCAAACCAATACCCAACACTTTATAGGGCG AATTGGAGCTC	This study
AG77R	TAACAACATCTTTCTCCATTCTCCATTCTCGACGGTATCGA	This study

	TAAGCTTGA	
AG78F	CCTATCCACATACATACACA	This study
AG78R	CGGACTTTGTAGTAATCAAG	This study
AG88F	ACCATCCACTTCAACTTACTTTTACACTTC	This study
AG88R	ACCATCCACTTCAACTTACTTTTACACTTC	This study
AG89F	GAGGAAAATGAAAGGGACCAATCTGTCTAT	This study
AG89R	TTCCCGGCTAGTTTTTATATCCAGTGGATT	This study
AG90F	ATCACTATCCCCTCCCTAAAAGAATAGTAGTATAGGGCGA ATTGGAGCTC	This study
AG90R	ATAGACAGATTGGTCCCTTTCATTTTCCTCGACGGTATCG ATAAGCTTGA	This study
AG91F	TGCTTCAAGACGTGACTTGG	This study
AG91R	CACTTACTCCAGAAAATAGC	This study
AG92F	ACACCAACAATGGTAATGGT	This study
AG92R	CTAGTCTTAGTTGGAGCAGA	This study
AG93F	AGCCAAACAGATACAGATAC	This study
AG93R	TTTAGGGAGGGGATAGTGAT	This study
AG99F	GACACACAAACAAACACCCC	This study
AG99R	AGGTTGGTTTGGTTTGCTCT	This study
AG115F	GGGTAAAGAG ATACCAAGAG	This study
AG115R	AGTGTAATGGGTTTAGTTGC	This study
AG101F	GTTGGGACTAGGATTGGTAAAGC	Carlisle and Kadosh, 2010
AG101R	GATGTGGAGTAGACTTGGATAATGG	Carlisle and Kadosh, 2010
HHHWP1F	CTAAACCAGCTGCTCCAAAAT	This study
HHHWP1R	GTTGTTACCAGCACCTTCAAA	This study
ACT1-129F	CATGGTTGGTATGGGTCAAAAA	This study
ACT1-104R	TCAATTCTAATAACGAGGTGGTCTTTC	This study
HH08F	TTCTGGCTCCAAATCATTTG	This study
HH08R	TATAAGGCTGCATAACTAAG	This study
HC10F	CGAGCAGGACCAATTGCGATGTAATCAAAATTGTTAACAT GAGTCTGTGTCTATTCGCCT ACTACTAACCTTAGAGTGTTGGATCCCCCCTTTAGTAAGA	This study
HC10R	GACAGGAGTAATGTTATTAGCTCTAGCATTGAGCTGGCCA CTATTCAATGGCTGTAAAGG TTGTGAACGAAGCGCCGACATGTTTTCTGGGGAGGGTA	This study
HC11F	ACTATGAATAGAGAAAGCAG	This study
HCGS13F	TCGAGCAGGACCAA TTGCGA TGT AA TCAAA	Chou *et al*., 2011
HCGS13R	GGTT AAACCTCTTT AA T AA TCAA TGCTGGT	Chou *et al*., 2011

HCGS14F	ACCAGCATTGATTATTAAAGAGGTTTAACCGGATCCCCCC TTTAGTAAGA	Chou *et al*., 2011
HCGS14R	CTGTAAAGGTTGTGAACGAAGCGCCGACATGTTTTCTGGG GAGGGTA	Chou *et al*., 2011
HCGS15F	ATGTCGGCGCTTCGTTCACAACCTTTACAG	Chou *et al*., 2011
HCGS15R	TAAAGAATCTAACCTCTGGTTCAGACACTC	Chou *et al*., 2011
HH43F	ATGGTTACACCCGATTCAAC	This study
HH08F	TTCTGGCTCCAAATCATTTG	This study
HH08R	TATAAGGCTGCATAACTAAG	This study
CaURA3F	GGTAATACCGTAAAGAAACA	This study
CaMET3R	TGGGGAGGGTATTTACTTTTAAAT	This study
CaARG4F	ACTATGGATATGTTGGCTAC	This study
CaHIS1R	ACTGGGATATCAGCTGCAGG	This study

Table 3: Plasmids used in this study

Name	**Source**
pRM1000	J. Pla
pBS-Ca*URA3*	A.P.J. Brown
pBS-Ca*HIS1*	C. Bachewich
pFA-*ARG4*-Met3p	Gola *et al*., 2003
pFA-HA-*URA3*	Lavoie *et al*., 2008
pFA-GFP-*URA3*	Gola *et al*., 2003

Table 4: Proportion (%) of different cell morphologies and corresponding frequency of tip-enriched filipin signal in different cell types[1].

	Unbudded	Small Bud[2]	Medium Bud[2]	Large Bud[2]	Elongated Bud[2]	Hyphae
30°C *cdc5/PCK1::CDC5*						
0 h (n=120)	59/0	1/1	33/0	5/0	2/0	0/0
2 h (n=120)	19/0	15/15	34/28	13.5/12	18.5/17	0/0
4 h (n=106)	0/0	0/0	0/0	0/0	100/96	0/0
6 h (n=101)	0/0	0/0	0/0	0/0	100/84	0/0
CDC5/CDC5						
0 h (n=106)	91/0	0/0	2/0	7/0	0/0	0/0
2 h (n=123)	34/11[3]	17/17	24/24	25/25	0/0	0/0
4 h (n=117)	10/7[3]	9.5/9.5	49.5/44.5	31/4	0/0	0/0
6 h (n=117)	22/6[3]	13/13	35/31	30/0	0/0	0/0
36°C *CDC5/CDC5*						
(n=110)	3/0	17/17	41/35.5	39/4.5	0/0	0/0
37°C + serum *CDC5/CDC5*						
(n=35)	0/0	0/0	0/0	0/0	0/0	100/98

[1]Strains AG240 (*cacdc5::hisG/cacdc5::HIS1 PCK1::CaCDC5-hisG, MLC1/MLC1-GFP-URA3*) and AG332 (*MLC1/MLC1-GFP-URA3*) were grown overnight at 30°C in inducing medium (SS), washed, diluted into repressing medium (SD) and incubated at 30°C for set times. Cells of strain AG332 were grown at 36°C for 4 h to promote pseudohyphal growth. Cells of strain AG332 were grown at 37°C with media supplemented with 10% FBS for 1.5 h to induce hyphal growth. Cells were stained with filipin for 10 min and analyzed by microscopy. Values represent percentage of cell morphology/percentage of those cells containing enriched filipin signal at a bud or filament tip.
[2]Buds scored as small were up to 0.25x in length that of the mother yeast cell, medium buds ranged from 0.25 to 0.5x the mother cell length, large buds were 0.5-1.0x the length of the mother yeast cell, and elongated buds contained lengths that were longer than that of the mother yeast cell.
[3]Non-budded cells with a polar spot of filipin signal on the surface.

Table 5: Mlc1p-GFP localization patterns in cells depleted of Cdc5p[1].

	Tip			Sub-apical			Tip + sub-apical[2]	
Cdc5p depletion (h)	Spot	Crescent	No signal	Bud-neck	Filament	No signal	Spot + bud-neck	Crescent + bud-neck
4 (n=107)	32.0	21.0	47.0	91.0	0	9.0	94.0	95.0
12 (n=58)	22.5	3.5	74.0	N.D.	17.5	82.5	15.4	0

[1]Strain AG240 (*cdc5::hisG/cdc5::HIS1 PCK1::CDC5-hisG, MLC1/MLC1-GFP-URA3*) was grown overnight at 30°C in inducing medium (SS), washed, diluted into repressing medium (SD) and incubated at 30°C for 4 or 12 h. Values are expressed as percentage of total cells.
[2] Of cells that contained signal in the tip, percentage that simultaneously showed signal in subapical regions.

Table 6: Filament diameter[1,2] in cells depleted of Cdc5p[3]

	cdc5Δ/MET3::CDC5			
CDC5 off (h)	*+/+*	*ume6Δ/ ume6Δ*	*hgc1Δ/ hgc1Δ*	*hmsΔ/ hms1Δ*
7	2.52±0.32	2.69±0.27 (p=0.01)	2.55±0.24 (p=0.65)	2.43±0.25 (p=0.10)
11	2.59±0.37	3.12±0.40 ($p=1.59x10^{-8}$)	2.91±0.35 ($p=4.17x10^{-5}$)	2.51±0.30 (p=0.21)

[1]Diameter measured 40 μm from the tip, ± s.e.m.

[2] Mean diameter of each deletion strain was compared to that of control strain AG553 using a Student's t-test (2 –tailed).

[3]Strains AG553 (*cdc5Δ::hisG/MET3::CDC5-ARG4, URA3+ HIS1),* AG530 (*cdc5Δ::hisG/MET3::CDC5-ARG4, ume6Δ::URA3/ume6Δ::HIS1*), AG574 (*cdc5Δ::hisG/MET3::CDC5-ARG4, hgc1Δ::URA3/hgc1Δ::HIS1*) and AG580 (*cdc5Δ::hisG/MET3::CDC5-ARG4, hms1Δ::URA3/hms1Δ::HIS1*) were diluted from inducing to repressing medium (+MC), incubated at 30°C for the indicated times and fixed. Approximately 50 cells were measured for each strain.

Table 7: Proportion (%) of cells stained with propidium iodide following *CDC5* repression[1]

	cdc5Δ/MET3::CDC5			
CDC5 off (h)	*+/+*	*ume6Δ/ ume6Δ*	*hgc1Δ/ hgc1Δ*	*hmsΔ/ hms1Δ*
7	5.8 (n=137)	7.8 (n=141)	3.5 (n=142)	3.8 (n=151)
11	15.8 (n=184)	18.7 (n=165)	16.6 (n=174)	15.4 (n=188)
15	25.6 (n=117)	55.4 (n=101)	35.8 (n=131)	38.9 (n=95)

[1] Strains AG553 (*cdc5Δ::hisG/MET3::CDC5-ARG4, URA3+ HIS1),* AG530 (*cdc5Δ::hisG/MET3::CDC5-ARG4, ume6Δ::URA3/ume6Δ::HIS1*), AG574 (*cdc5Δ::hisG/MET3::CDC5-ARG4, hgc1Δ::URA3/hgc1Δ::HIS1*) and AG580 (*cdc5Δ::hisG/MET3::CDC5-ARG4, hms1Δ::URA3/hms1Δ::HIS1*) grown in inducing medium (-MC) were diluted into repressing medium (+MC) and incubated at 30°C for the indicated times. Live cells were stained with propidium iodide (PI), washed with sterile water, and immediately examined by fluorescence microscopy.

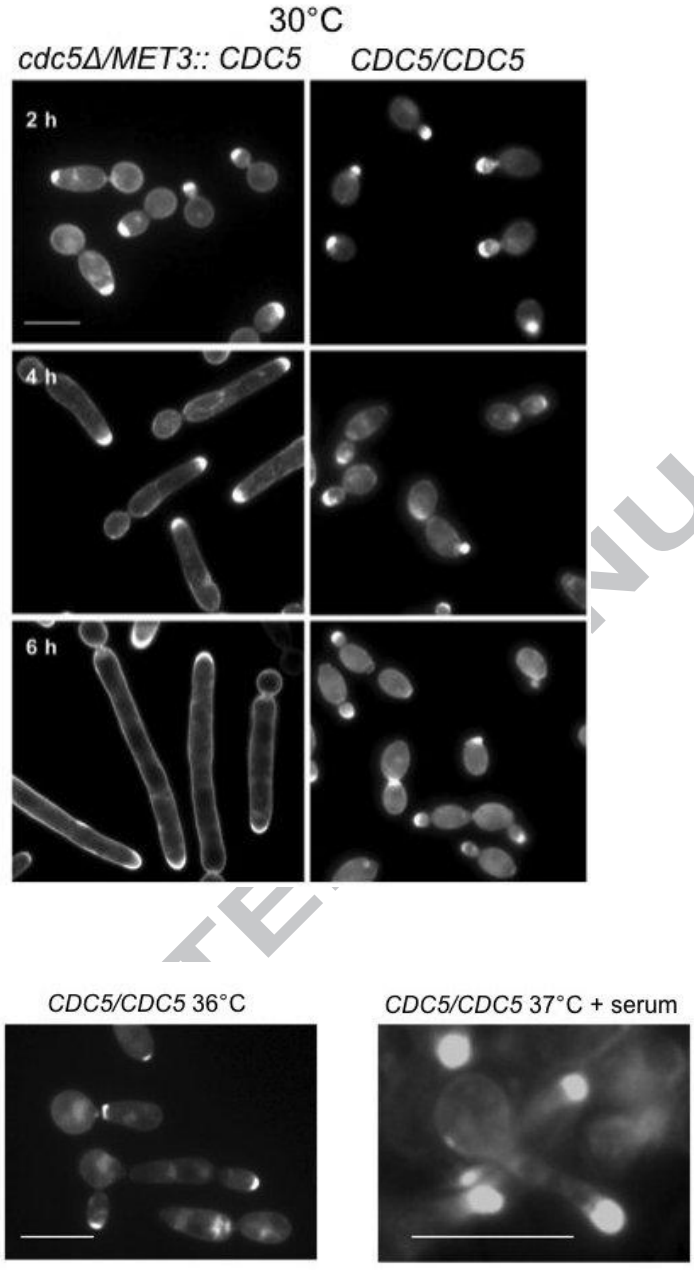
30°C
cdc5Δ/MET3:: CDC5
CDC5/CDC5
2 h
4 h
6 h
CDC5/CDC5 36°C
CDC5/CDC5 37°C + serum

Fig. 1

A

Mlc1p-GFP FM4-64 MERGE

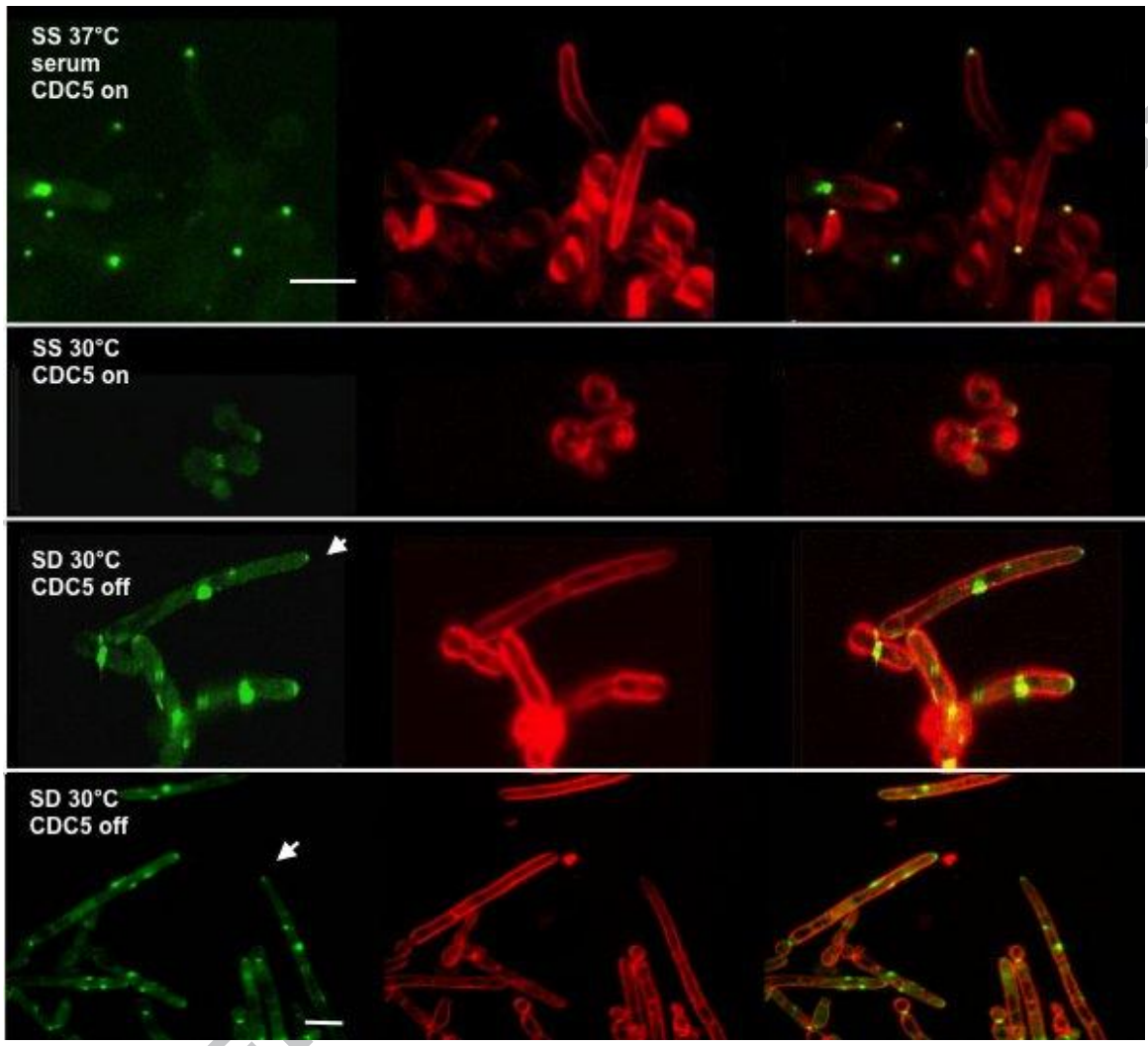

Mlc1p-GFP FM4-64 MERGE

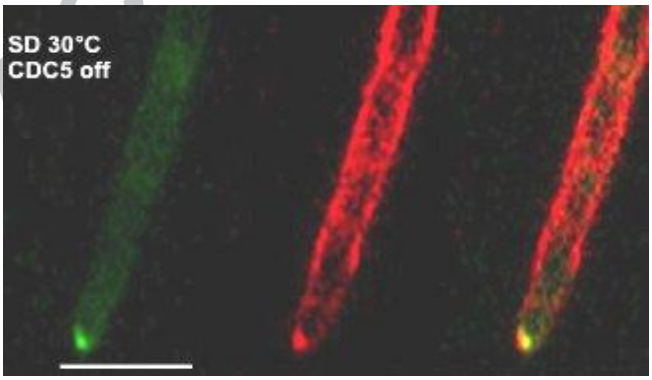

Fig. 2

C

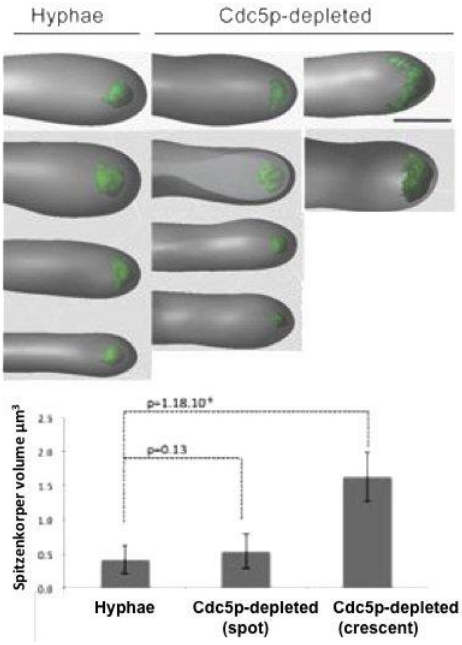
Hyphae
Cdc5p-depleted
p=1.18.10⁻⁴
p=0.13
Spitzenkorper volume µm³
Hyphae
Cdc5p-depleted (spot)
Cdc5p-depleted (crescent)

D

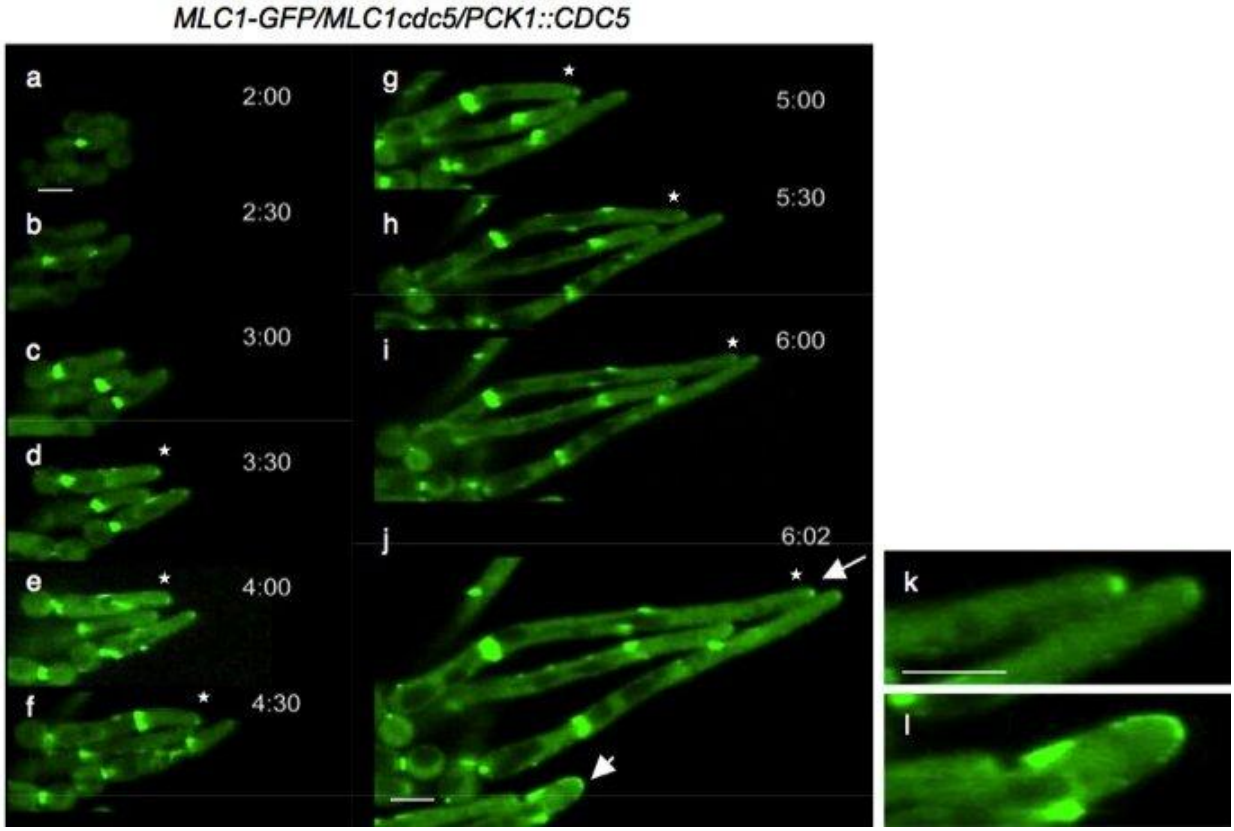
MLC1-GFP/MLC1cdc5/PCK1::CDC5
a 2:00
b 2:30
c 3:00
d 3:30
e 4:00
f 4:30
g 5:00
h 5:30
i 6:00
j 6:02
k
l

Fig. 2

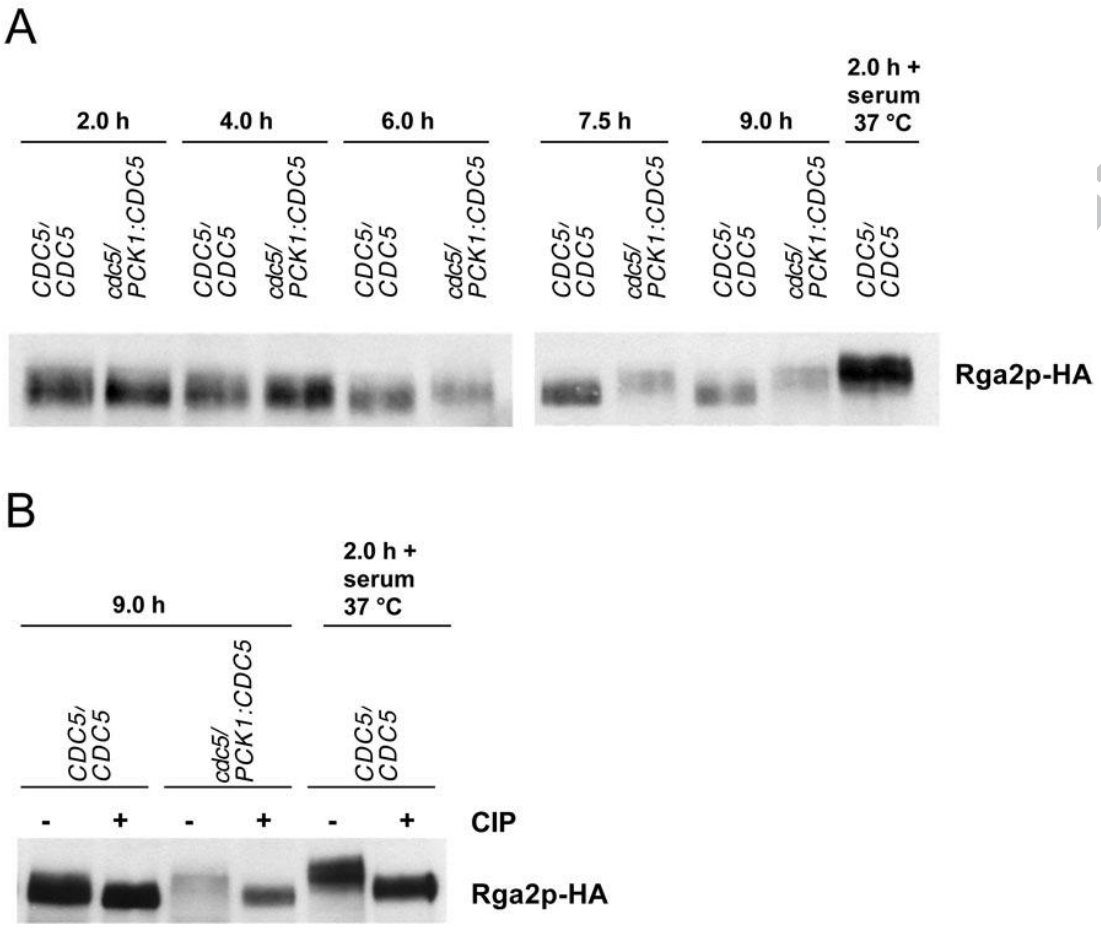

Fig. 3

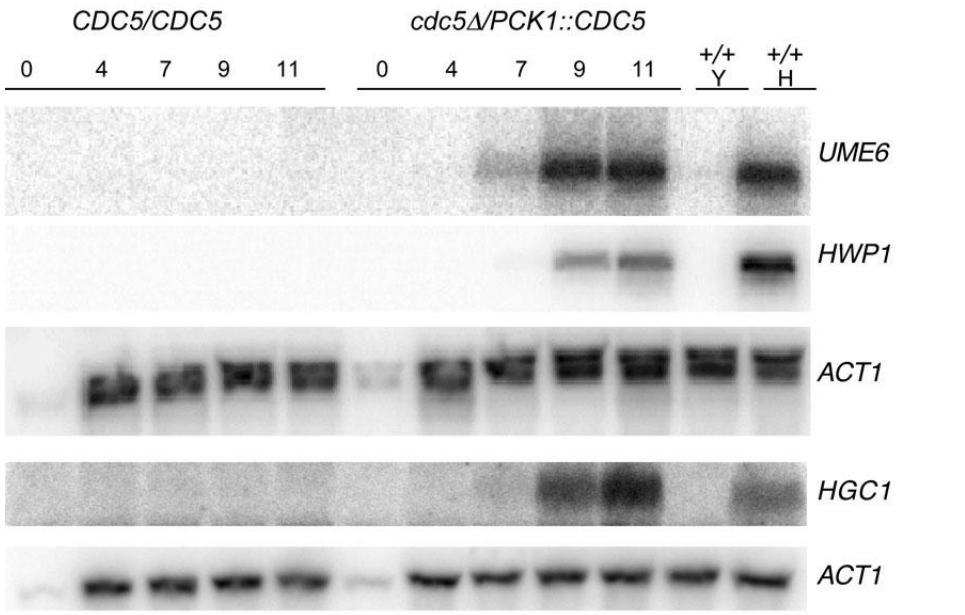

						Rel. Density
1.0	3.7	7.0	6.1	-	7.7	*UME6*
1.0	29.1	151.6	375.3	-	526.3	*HWP1*
1.0	8.7	52.2	65.3	-	39.8	*HGC1*

Fig. 4

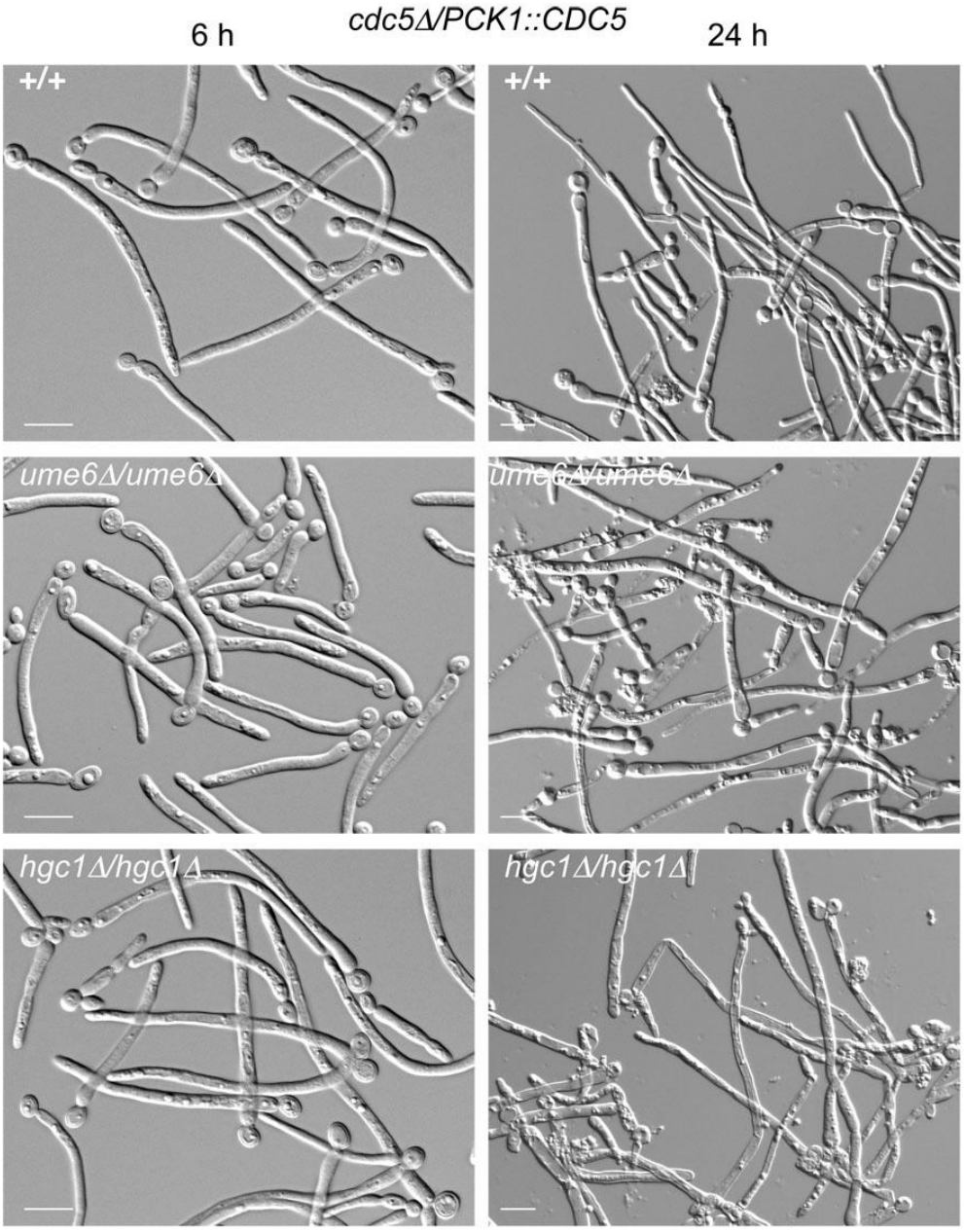
cdc5Δ/PCK1::CDC5
6 h
24 h
+/+
+/+
ume6Δ/ume6Δ
ume6Δ/ume6Δ
hgc1Δ/hgc1Δ
hgc1Δ/hgc1Δ

Fig. 5

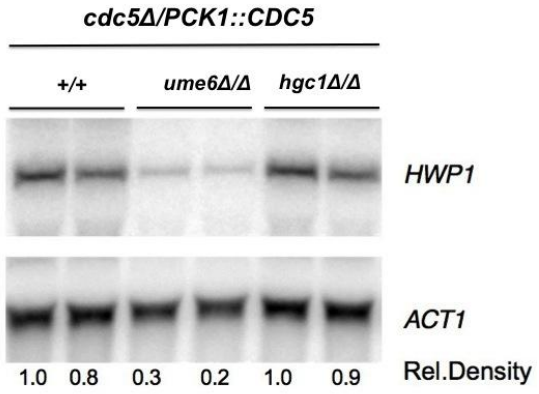
cdc5Δ/PCK1::CDC5
+/+
ume6Δ/Δ
hgc1Δ/Δ
HWP1
ACT1
1.0 0.8 0.3 0.2 1.0 0.9
Rel.Density

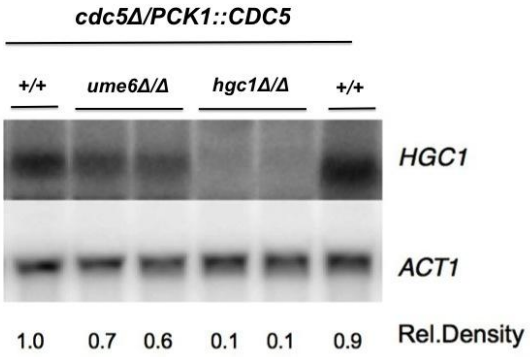
cdc5Δ/PCK1::CDC5
+/+
ume6Δ/Δ
hgc1Δ/Δ
+/+
HGC1
ACT1
1.0 0.7 0.6 0.1 0.1 0.9
Rel.Density

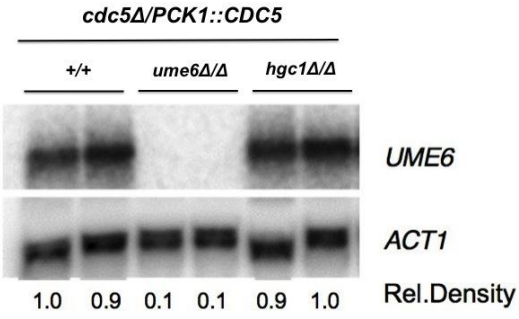
cdc5Δ/PCK1::CDC5
+/+
ume6Δ/Δ
hgc1Δ/Δ
UME6
ACT1
1.0 0.9 0.1 0.1 0.9 1.0
Rel.Density

Fig. 6

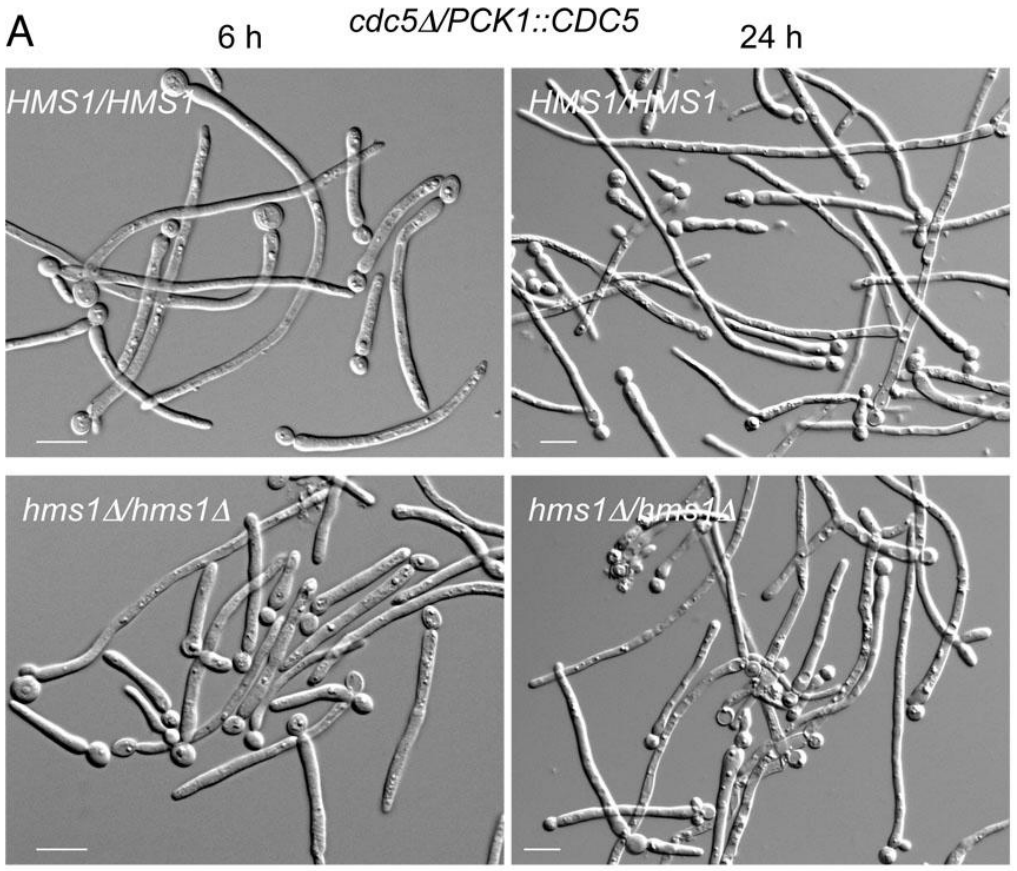
A
6 h
cdc5Δ/PCK1::CDC5
24 h
HMS1/HMS1
HMS1/HMS1
hms1Δ/hms1Δ
hms1Δ/hms1Δ

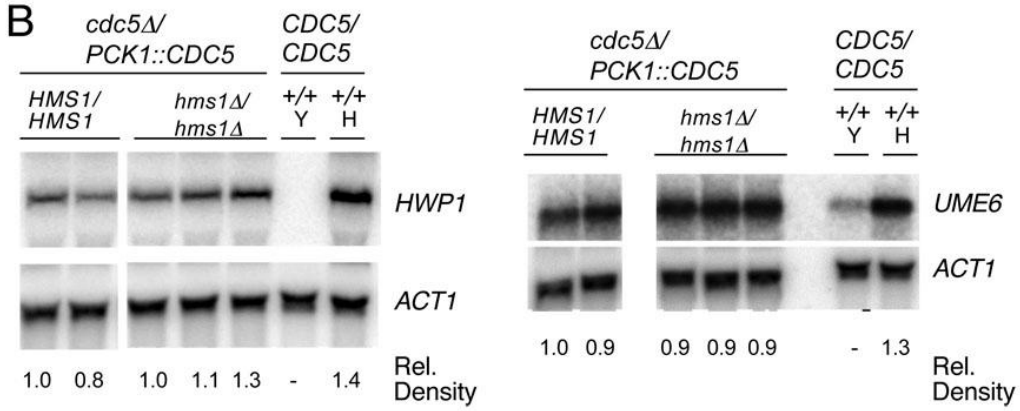
B
cdc5Δ/ PCK1::CDC5
CDC5/ CDC5
HMS1/ HMS1
hms1Δ/ hms1Δ
+/+ Y
+/+ H
HWP1
ACT1
1.0 0.8 1.0 1.1 1.3 - 1.4
Rel. Density
cdc5Δ/ PCK1::CDC5
CDC5/ CDC5
HMS1/ HMS1
hms1Δ/ hms1Δ
+/+ Y
+/+ H
UME6
ACT1
1.0 0.9 0.9 0.9 0.9 - 1.3
Rel. Density

Fig. 7

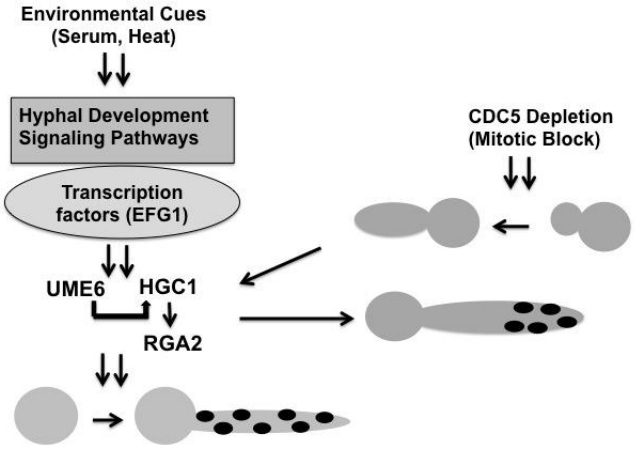

Fig. 8